Diplomarbeit

ANTI-TUMOR EFFECTS OF METABOTROPIC GLUTAMATE RECEPTOR 1 ANTAGONISTS ON NEUROENDOCRINE TUMOR CELL LINES

eingereicht von

Katharina Rohrer

Geb.Dat.: 02.03.1990

zur Erlangung des akademischen Grades

Doktorin der gesamten Heilkunde

(Dr. med. univ.)

an der

Medizinischen Universität Graz

ausgeführt am

Institut für Pathophysiologie und Immunologie

unter der Anleitung von

Univ.-Ass. Mag. Dr.rer.nat. Nassim Ghaffari Tabrizi-Wizsy

Ao.Univ. Prof.i.R. Dr.phil. Roswitha Pfragner

Graz, am 5. Juni 2014 Katharina Rohrer

Eidesstattliche Erklärung

Ich erkläre ehrenwörtlich, dass ich die vorliegende Arbeit selbstständig und ohne fremde Hilfe verfasst habe, andere als die angegebenen Quellen nicht verwendet habe und die den benutzten Quellen wörtlich oder inhaltlich entnommenen Stellen als solche kenntlich gemacht habe.

Graz, am 5. Juni 2014 *Katharina Rohrer*

Statutory Declaration

I declare that I have authored this thesis independently, that I have not used other than the declared sources / resources, and that I have explicitly marked all material which has been quoted either literally or by content from the used sources.

Graz, am 5. Juni 2014 *Katharina Rohrer*

ACKNOWLEDGMENT

I am deeply indebted to Mag. Dr. Nassim Ghaffari Tabrizi-Wizsy for her valuable guidance and continuous support in the process of writing this thesis. Her efforts encouraged me to broaden my knowledge and paved my way into the wide area of research.

I wish to express special appreciation to Prof. Dr. Roswitha Pfragner for welcoming me in her lab and providing support for all experiments. I would like to thank Dr. Gert Schwach for teaching me cell culturing.

Furthermore, I am grateful to Prof. Dr. Anton Sadjak, the head of the Institute of Pathophysiology and Immunology, for the provision of research infrastructure and his encouragement for research and training.

Special thanks go to MA Helga Haas for assisting me in designing the experiments, for helping me to conduct statistical analysis, and for reviewing this work. Without her persistent help this thesis would not have been possible.

I wish to thank Charlotte Horwath and Elke Schwarzenberger for providing technical assistance in the cell culture lab. I am grateful to Nathalie Meier-Allard who taught me PCR and who was always available and willing to answer all questions I came up with.

Additionally, I would like thank my colleagues at the lab for creating a friendly atmosphere that made working here very enjoyable.

Last but not least, I would like to thank my parents for their financial and mental support during my medical studies that come to a close with the thesis at hand.

ZUSAMMENFASSUNG

Einleitung: Karzinoide des Dünndarms (SI-NETs), sowie medulläre Schilddrüsenkarzinome (MTCs) zählen zur Gruppe der Neuroendokrinen Tumoren (NETs). Die Inzidenz dieser Tumoren ist in den letzten Jahren gestiegen, jedoch sind die Behandlungsmöglichkeiten weiterhin beschränkt. Da die Tumoren nur gering auf Chemo- und Strahlentherapie ansprechen, sind radikale chirurgische Verfahren die einzige kurative Behandlungsmöglichkeit. Glutamat, ein exzitatorischer Neurotransmitter, spielt nicht nur im zentralen Nervensystem eine wichtige Rolle, sondern auch in peripheren Geweben. Glutamatrezeptor Antagonisten unterdrücken das Wachstum unterschiedlicher maligner Zellen (z.B. Melanomzellen, Brustkrebszellen). In dieser *in vitro* Studie wurde das therapeutische Potential von nicht kompetitiven, subtyp-spezifischen Antagonisten des metabotropen Glutamatrezeptors 1 (mGluR1) in der Behandlung von NETs analysiert.

Material und Methoden: Vier SI-NET Zelllinien (KRJ-I, P-STS, L-STS, H-STS) und zwei MTC Zelllinien (MTC-SK, SHER-I) wurden mit unterschiedlichen Konzentrationen (10– 200 µM) von zwei mGluR1 Antagonisten (Cyclothiazide und YM-298198) behandelt. Nach 24, 48 und 72 h Inkubation wurden die Zellen lichtmikroskopisch beurteilt sowie deren Zellzahl, Zellgröße und die metabolischen Aktivität (mittels WST-1 Assay) bestimmt. Zusätzliche wurden die Substanzen in Kombination mit dem Chemotherapeutikum Temozolomide (TZM) getestet.

Ergebnisse: Beide mGluR1 Antagonisten zeigen dosisabhängige Effekte auf Zellwachstum und metabolische Aktivität, wobei die Dosis von 200 µM am stärksten wirkt. Die Ergebnisse der Kombinationsversuche mit TZM weisen auf einen synergistischen Effekt sowohl bezüglich der Zellzahl, als auch der metabolischen Aktivität hin. Außerdem konnte die Expression von mGluR1 in allen Zelllinien nachgewiesen werden.

Schlussfolgerungen: Die erhobenen Daten zeigen, dass mGluR1 Antagonisten Einfluss auf Wachstum und Metabolismus von NET Zellen haben und daher als neue Behandlungsmöglichkeit in Frage kommen könnten. Diese *in vitro* Studie bildet die Grundlage für weitere Untersuchungen zur genaueren Evaluierung des therapeutischen Potentials, sowie für ein besseres Verständnis der Tumorbiologie von Neuroendokrinen Tumoren.

ABSTRACT

Introduction: Small intestinal neuroendocrine tumors (SI-NETs) and medullary thyroid carcinomas (MTC) are counted among the neuroendocrine tumors (NETs). In recent years, the incidence of these tumors has been increasing, but treatment options are still limited. As NETs show low response rates to radiation and chemotherapy, radical surgery still is the only curative therapy option. Glutamate, an excitatory neurotransmitter, plays an important role not only in the central nervous system, but also in peripheral tissues. Glutamate antagonists reduce proliferation of different malignant cells (e.g. melanoma cells, breast cancer cells). In this *in vitro* study the therapeutic potential of non-competitive, subtype-specific metabotropic glutamate receptor 1 (mGluR1) antagonists in treatment of NETs was analysed.

Material and methods: Four SI-NET cell lines (KRJ-I, P-STS, L-STS, H-STS) and two MTC cell lines (MTC-SK, SHER-I) were treated with different concentrations (10- 200 µM) of two mGluR1 antagonists (Cyclothiazide and YM-298198). After 24, 48 or 72 h of incubation, light microscopy, cell counting and analysing as well as analysis of the metabolic cell activity by the WST-1 assay were performed. Additionally, the substances were tested in combination with the chemotherapeutic agent Temozolomide.

Results: Both mGluR1 antagonists show dose dependent effects on cell growth and metabolic activity, whereby the dosage of 200 µM was the most effective. The results of the combined treatment with TZM indicate a synergistic effect concerning cell counts and metabolic activity. Furthermore, expression of mGluR1 was detected in all tested cell lines.

Conclusion: These data show that mGluR1 antagonists influence growth and metabolism of NET cells. Therefore they could be a new treatment option. This *in vitro* study builds the basis for further investigations to evaluate the therapeutic potential of mGluR1 antagonists and for a better understanding of the tumor biology of neuroendocrine tumors.

TABLE OF CONTENTS

A. INTRODUCTION

1. Neuroendocrine tumors

Neuroendocrine tumors (NETs) originate from neuroendocrine cells which derive from the embryonic neural crest, ectoderm and endoderm, and build a heterogeneous group of rare neoplasms developing at many sites of the body. Although NETs can occur in any location containing neuroendocrine cells (e.g. testis, ovary, salivary glands or the carotid body), NETs of the gastrointestinal system are the most common (67%). Most NETs appear sporadically, but there is also an association to genetic syndromes (e.g. multiple endocrine neoplasia 1 (MEN1)) (1).

Incidence of NETs shows a significant increase from 1973 (1.09/100,000) to 2004 (5.25/100,000) (Fig. 1.). Several factors can predict the outcome, e.g. disease stage, histopathology and primary tumor site. Over time there was no significant improve of survival duration among patients with localised NETs, but a high significant enhancement of the survival duration among patient with metastatic disease diagnosed after introduction of octreotide in 1987. However, radical surgery still is the only curative treatment option (2).

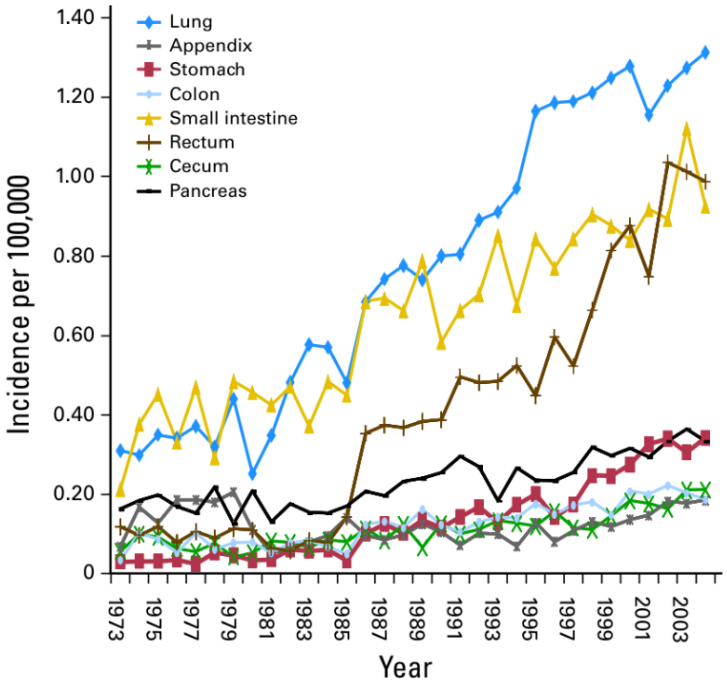

Fig. 1 - Increasing incidence of neuroendocrine tumors over time
[taken from (2)]

1.1 Small intestinal neuroendocrine tumors

NETs of the gastrointestinal system derive from serotonin producing enterochromaffin cells (EC). In case of metastasis, secretion of bioactive substances can lead to the characteristic clinic symptoms of the carcinoid syndrome (flushing, diarrhea, heart valvular lesions and abdominal cramping). Many NETs are initial clinically silent until increased tumor mass causes local symptoms (e.g. a vague abdominal pain), which are unspecific and often misinterpreted (1). Small intestinal neuroendocrine tumors (SI-NETs) form the most common group of NETs (25,2%). 58-64% of all patients present with metastatic disease at the time of their initial diagnosis (3). Until now, radical surgery of localized disease is the only curative treatment option, but surgery is suitable only to 20% of patients (4,5). As conventional chemotherapy and external radiotherapy does not show efficient effects, therapy is symptom-orientated. Somatostatin analogues (e.g. octreotide) can be used to improve quality of life (5). Because therapy options are still insufficient and SI-NETs show increasing incidence, there is need to develop new strategies for antitumor therapy.

1.2 Medullary thyroid carcinoma

Medullary thyroid carcinomas (MTCs) are rare malignancies that derive from calcitonin-secreting parafollicular C-cells of the thyroid gland which originate from the neural crest (6). They occur in sporadic and autosomal dominant inherited forms (20-25%). Hereditary MTC syndromes, caused by mutations in the rearranged during transfection (RET) proto-oncogene, are divided into MEN 2A (Sipple's syndrome), familiar MTC (FMTC), and MEN 2B (7). Untreated MTCs have a high morbidity and mortality. First line treatment is radical surgery (total thyroidectomy and central lymph node dissection). Palliative care includes radiation, chemotherapy and targeted therapies (e.g. inhibition of tyrosine kinase and vascular endothelial growth factor receptors) (8).

1.3 New therapy concepts in the treatment of NETs

Standard drug therapy is limited. In case of SI-NET, it usually consists of a treatment with a somatostatin analoga. Recent studies suggest mammalian target of rapamycin (mTOR) inhibitors (e.g. Temsirolimos), vascular endothelial growth factor (VEGF) blockers as

Bevacizumab and epidermal growth factor receptor (EGFR) inhibitors as Gefitinib as new possible therapy options. However, there is a high interest to investigate therapy options (9).

1.4 Glutamate signalling

In the early 1950s research about glutamate signalling and its role in transmission and disease began. The nonessential amino acid L-glutamate is known as the major excitatory neurotransmitter of the central nervous system (CNS) and participates in many neural functions (10,11). Glutamate is approved to play a role in the pathogenesis of human neurological and neurodegenerative psychiatric disorders (e.g. anxiety and schizophrenia). Glutamate receptors (GluRs) are not only expressed in the CNS, but also in peripheral, non-excitable cells (bone osteoblasts and osteoclasts, keratinocytes, megakaryocytes, pancreatic isle cells, the lung, the liver, the heart, kidney cells, adrenal tissue, immune tissue and taste buds) (12). Glutamate plays a role as an extracellular signal mediator in the autocrine and/or paracrine system in peripheral tissues (13).

1.5 Glutamate receptors

Glutamate stimulates more than twenty receptors which are divided into two families: Ionotropic and metabotropic glutamate receptors (iGluRs and mGluRs) (Fig. 2) (14,15).

Ionotropic glutamate receptors

iGluRs are ligand-gated cation channels, which are permeable to Na^+, K^+ and Ca^{2+}. This group of receptors is further subdivided into three subfamilies, based on selective agonists: N-methyl-D-aspartate (NMDA), α-amino-3-hydroxy-5-methyl-4-isoazolepropionic acid (AMPA) and 2-carboxy-3-carboxymethyl-4-isopropenylpyrrolidine (kainate) receptors (14,15).

Metabotropic glutamate receptors

Eight members of the metabotropic glutamate receptors (mGluR1-8) family are identified which are all G-protein-coupled. Further categorization, on the basis of sequence homology, pharmacology and transduction, divides three groups of mGluRs. Group I receptors (mGluR1 and mGluR5) are coupled to Gq proteins. Activation leads to signalling cascades involving phospholipase C (PLC), inositol 1,4,5-trisphosphate (IP3) and

diacylglycerol (DAG). Group II receptors (mGlu2 and mGlu3) and Group III receptors (mGluR4, mGluR6, mGluR7 and mGluR8) are coupled to Gi proteins, which are negatively linked to adenylate cyclase and decrease cyclic adenosine monophosphate (cAMP) levels (14-16).

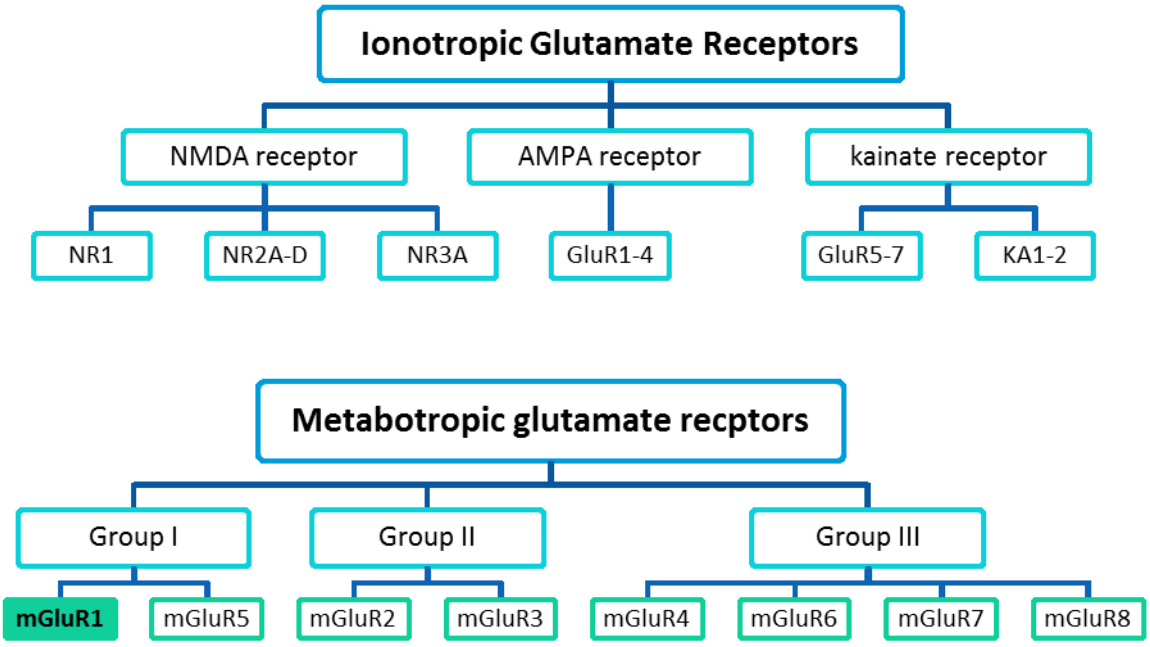

Fig. 2 - Overview of the glutamate receptor family
Ionotropic glutamate receptors (iGluRs) and metabotropic glutamate receptors (mGluRs) are further subdivided. mGluR1 is the target of the study. [taken from (14), modified]

2. mGluR1 as target

2.1 mGluR receptors

All mGluRs are guanine nucleotide-binding protein (G-protein)-coupled receptors (GPCRs), belonging to the C GPCR family. Besides, this receptor family contains the $GABA_B$, Ca^{2+}-sensing, pheromone and taste receptors and share following structural similarities. Characteristic is a large extracellular N-terminal domain, containing the venus flytrap domain (VFT), where the endogenous agonists (e.g. glutamate) binding site is localized, and a cysteine-rich domain (CRD). Furthermore, a seven transmembrane domain is typical as well as a variable-length intracellular C-terminal domain (Fig. 3) (15,16).

Dimerization of the N-terminal domains let the mGluRs appear as homodimers (16). This dimerization is stabilized by intermolecular disulfide bonds and seems to play a critical role in activation of the receptors. Full activation requires agonists binding to both N-terminal domains (17,18).

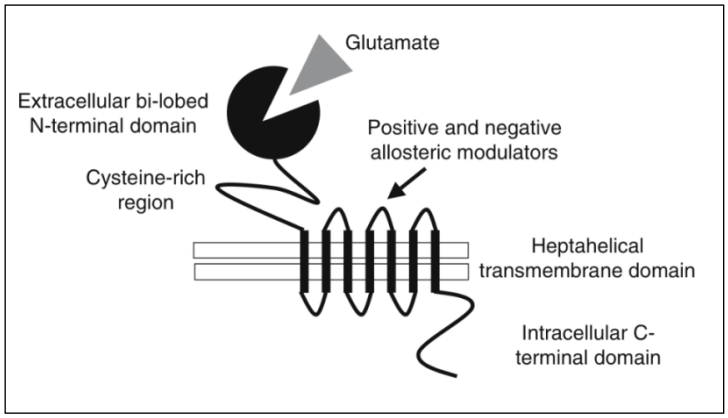

Fig. 3 - The structure of metabotropic glutamate receptors
N-terminal domain, the seven transmembrane spanning regions and the C-terminal domain, as well as glutamate binding at the N-terminal domain and binding site of allosteric modulators. [taken from (15)]

2.2 mGluR1 signalling

As mentioned above, mGluR1s are generally coupled to Gq proteins. Stimulation of mGluR1s activates phospholipase C, followed by hydrolysis of phosphotinositides and generation of IP3 and DAG, two second messengers. Subsequently, PKC gets activated followed by increased Ca^{2+} release from intracellular stores (15).

Beneath this classical pathway other cascades are approved, including Gi and Gs protein activation, but also G protein independent signalling e.g. activation of coupled ion channels, mitogen activated protein kinase (MAPK) and extracellular-signal related kinase (ERK). Fig. 4 shows alternative pathways (15). Aditionally, modulation of the mGluR1 by the extracellular cation Ca^{2+} is described (19).

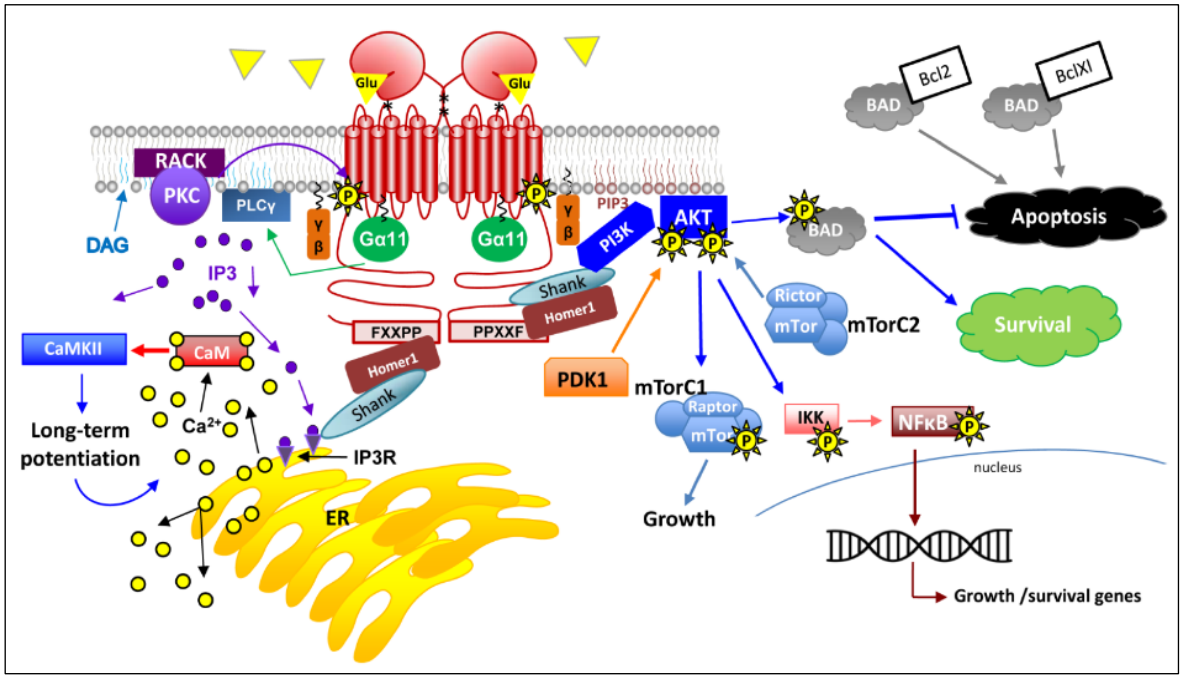

Fig. 4 - Signalling pathways activated by mGluR1 [taken from (15)]
Following second messenger systems play a role in glutamate (Glu) signalling: protein kinase C (PKC), diacylglycerol (DAG) and inositol 1,4,5-trisphosphate (IP3) work together to release intracellular Ca^{++} from the endoplasmic reticulum (ER). Ca^{++} binds to calmodulin (CaM), a second messenger. Homer 1 protein and the scaffold protein Shank interact via (PI3K) with AKT, also known as proteinkinase B (PKB). The PI3K/AKT/mTorC1 and 2 (phosphatidylinositol-4,5-bisphosphate 3-kinase, mammalian target of rapamycin complex 1 and 2) pathway plays a critical role in cell growth and cancer. NFκB (nuclear factor kappalight-chain-enhancer of activated B cells) also is involved in cell growth processes. Phosporylation (P) of Bcl2-associated death protein (BAD) leads to dissociation from the complex with the B-cell lymphoma 2 (Bcl2) complex. This causes an antiapoptotic effect (15).

2.3 mGluR1 antagonists

mGluR1 antagonists can be divided into competitive ligands interacting with the N-terminal, like orthosteric agonists do, and noncompetitive ligands (20).

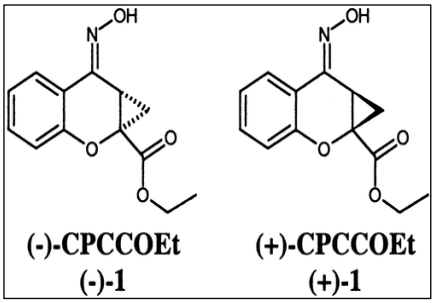

Fig. 5 - Chemical structure of racemic CPCCOEt
[taken from (21)]

CPCCOEt (7-(hydroxyimino)cyclopropa[b]chromen-1a-carboxylate ethyl ester) (Fig. 5) is the first detected noncompetitive mGluR1 antagonist, which interacts with the Thr-815 and Ala-818 residues on the transmembrane segment VII. CPCCOEt selectively inhibits the mGluR1 without affecting glutamate binding (21,22,22).

Cyclothiacide (CTZ) (3-(5-bicyclo[2.2.1]hept-2-enyl)-6-chloro-1,1-dioxo-3,4-dihydro-2H-1λ6,2,4-benzothiadiazine-7-sulfonamide) and YM-298198 (YM) (6-amino-N-cyclohexyl-N,3-dimethylthiazolo[3,2-a]benzimidazole-2-carboxamide) are mGluR1 antagonists (Fig. 6) which interact in a noncompetitive manner with the common allosteric binding site like the prototypic noncompetitive antagonist CPCCOEt does. CTZ and YM selectively inhibit mGluR1 and do not interact with other mGluRs (23,24). However, CTZ showed suppression of desensitization of AMPA receptors (25).

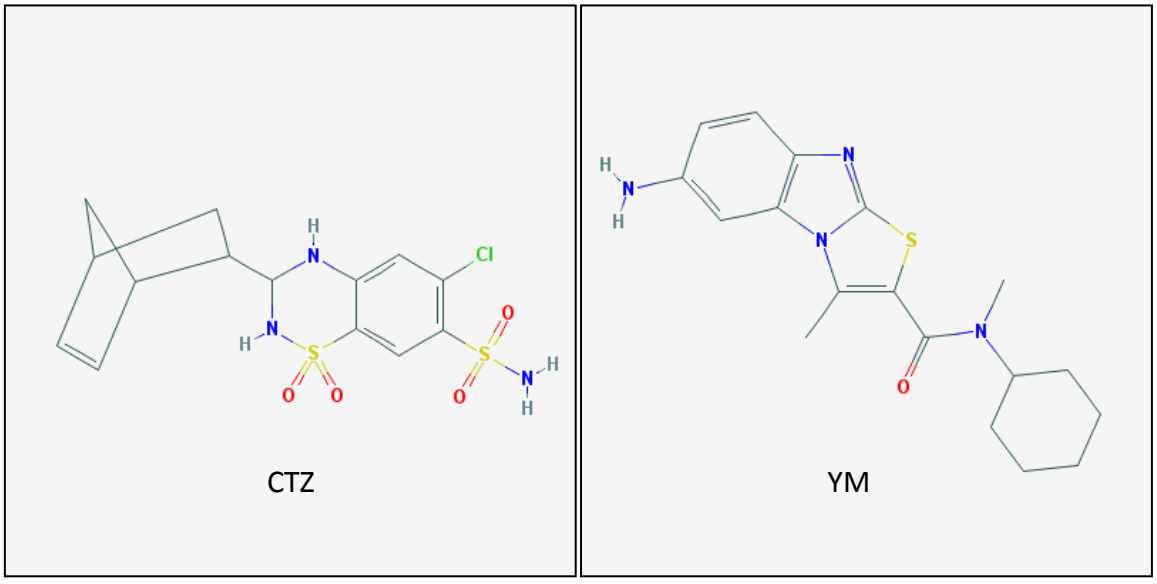

Fig. 6 - Chemical structure of the noncompetitive mGluR1 antagonists CTZ and YM
[taken from https://pubchem.ncbi.nlm.nih.gov/]

2.4 mGluR1 and tumor growth

For a long time, expression of mGluRs has been described only in the central nervous system. mGluR signalling is involved in several neuronal functions and disorders (e.g. learning and memory, nociception and depression). Modulation of mGluR signalling is implicated in the pathogenesis of different neuronal disorders (e.g. epiley, parkinson's disease, anxiety and schizophrenia) (20). Later, expression of mGluRs in peripheral tissues has been found, suggesting a functional role in non-neuronal cells (26). Further investigations show mGluR expression in cancer, not only in neuronal tumors (e.g. neuroblastoma, glioma and medulloblastoma) but also in tumors of non-neuronal tissues (e.g. melanoma and breast cancer) (12,27). Glutamate receptor antagonists inhibit tumor growth of colon adenocarcinoma, breast and lung carcinoma cells *in vitro* and improve effects of common chemotherapeutic agents used in cancer therapy (28). Expression of mGluR1 is detected in prostate cancer cells, but interestingly not in normal glands. Additionally, higher glutamate serum levels in patients with prostate cancer correlate to the Gleason grading system, which is used to evaluate prognosis (29). Consequently, mGluR1 as new target for cancer therapy is object of many investigations (30).

mGluR1 and melanoma cells

mGluR1 signalling plays a critical role in the pathogenesis of malignant melanomas. Metastatic melanomas showed upregulated mGluR1 expression (31). mGluR1 expression was detected in several human melanoma biopsies and cell lines, but not in nevi and melanocytes. Characterization of a novel mouse melanoma model pointed out that ectopic mGluR1 expression participates in melanogenesis and metastasis (32). In continuation of these experiments Haas et al. described attenuation of cell proliferation and mitochondrial activity in HBMC and n15006 melanoma cells after treatment with the mGluR1 antagonist CPCCOEt alone, and an enhancement of the antiproliferative effects after combined administration of CPCCOEt and the cytostatic drug docetaxel (33).

mGluR1 and breast cancer

mGluR1 expression was detected in five triple negative breast cancer (TNBC) cells and inhibition of tumor growth was described after treatment with the noncompetitive mGluR1 antagonists BAY36-7620 ((3aS,6aS)-6a-naphthalen-2-ylmethyl-5-methyliden-

hexahydro-cyclopental[c]furan-1-on) and Riluzole (6-(trifluoromethoxy)-1,3-benzothiazol-2-amine), *in vitro* and *in vivo* (MDA-MB-231 xenograft model) (34).

mGluR1 and neuroendocrine tumors

Little is known about glutamate signalling in NETs, but recent data indicate that the noncompetitive, subtype-specific, mGluR1 antagonist CPCCOEt causes inhibition of tumor growth in MTC cell line MTC-SK (35).

First results demonstrate the noncompetitive specific mGluR1 antagonists as possible new treatment option. Further investigations are required to evaluate mGluR1 as a new target in cancer therapy.

3. Temozolomide

The alkylating chemotherapeutic agent Temozolomide (TZM) is an imidazotetrazine derivative of dacarabazine and shows a broad spectrum of antitumor activity (Fig. 7) (36,37).

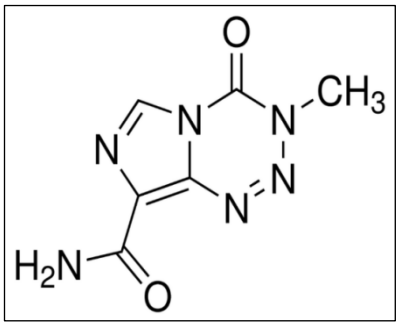

Fig. 7 - Chemical structure of Temozolomide (C6H6N6O2) [taken from http://www.sigmaaldrich.com/catalog/product/sigma/t2577?lang=de&region=AT]

Since approval in 1999, TZM is used for therapy of tumors in the central nervous system (e. g. glioblastoma multiforme) (36). Prolonging effects on survival of patients with glioblastoma multiforme after treatment with TZM in association with radiotherapy are described in several publications (38,39). More recently, TZM also received attention in the treatment regimens of several other tumors (36). In treatment of metastatic melanoma, TZM shows comparable therapeutic effects to the most common used chemotherapeutic agent dacarbazine, with the advantage of being an oral treatment (37,40).

Additionally, TZM has therapeutic potential in the treatment of NETs. Several publications show improvement of progression free survival of patients with NETs, treated with TZM alone or in association (e.g. bevacizumab, somatostatin analogue, capecitabine) (41-45).

4. Aims of the study

Treatment regimens for NETs are still insufficient and new therapy strategies are needed. mGluR1 antagonists are capable to supress tumor growth and cell activity of different peripheral malignancies. The aim of this study was to examine the effects of

- single treatment with mGluR1 antagonists (Cyclothiazide and YM-298198) and
- combined treatment with aforementioned mGluR1 antagonists and the chemotherapeutic agent Temozolomide

on proliferation, cell size and metabolic activity of

- four small intestinal neuroendocrine tumor cell lines (KRJ-I, P-STS, L-STS and H-STS) and
- two medullary thyroid carcinoma cell lines (MTC-SK and SHER-I).

B. MATERIAL AND METHODS

1. Cell lines

1.1 SI-NETs cell lines

KRJ-I

The KRJ-I cell line was derived from the primary tumor of a small intestinal carcinoid of a 75-year old Caucasian male. This cell line, growing in a suspension culture with a doubling time of two days, consists of single cells and cell spheroids. Cytogenetic analysis reported clonal tetraploidy and clonal loss of the Y chromosome (46). Further investigations confirmed the presence of neuroendocrine characteristics such as the presence of serotonin (5-HT) positive cytoplasmatic vesicles as well as the secretion of 5-HT. In addition, typical transcripts e.g. for chromogranin A, VMAT1, tryptophan hydroxylase, substance P, guanylin and SERT were detected by RT-PCR (47).

P-STS, H-STS, L-STS

P-STS, H-STS and L-STS cells were established from a SI-NET of a 42-year old man by Pfragner et al. (2009). P-STS cells originated from the primary tumor and appeared in a slackly monolayer together with detached cell spheroids with a doubling time of four days. H-STS and L-STS cells, which were derived from hepatic and lymph node metastases, grew as cell spheroids in suspension culture and showed a doubling time of three and two days. Immunocytochemical analysis showed expression of NET-markers (5-HT, calcitonin and gastrin-releasing factor) in variable frequency and intensity. Neuroendocrine granules were detected by electron microscopy. Cytogenetic analyses confirmed numeral and structural chromosomal abnormalities. All three cell lines showed tumorigenous properties after injection in SCID-mice (48).

1.2 MTCs cell lines

MTC-SK

The cell line MTC-SK was derived from a primary tumor of a sporadic MTC of a 51-year-old woman and was established by Pfragner et al. (1990). After detachment of a previous

formed monolayer, MTC-SK cells appear in spheroid formation. Compared to the original tissue, cultured cells contained less neuroendocrine granules. Further examinations (in situ hybridization and immunohistochemistry) confirmed persisting of neuroendocrine features such as the production of calcitonin, calcitonin gene-relate peptide and gastrin-releasing peptide. Expression of serotonin could not be found. Cytogenetic analysis showed terminal chromosomal rearrangements regarding chromosome 11p, where the calcitonin and calcitonin gene-related peptide genes are located (49).

SHER-I

The cell line SHER-I, which was established by Pfragner et al. (2008), originated from a primary tumor of a medullary thyroid cancer. This cell line grows in suspension culture with single cells and cell spheroids. Cells show a low telomerase activity (49,50).

1.3 HF-SAR

HF-SAR cells were established from skin of a two year old male. This normal human skin fibroblasts grow adherent (personal communication R. Pfragner).

2. Gene expression of mGluR1

2.1 RNA Isolation

To isolate RNA TriReagent RT (Molecular Research Center Inc., Cincinnati, USA), a single-step reagent for RNA isolation, was used according to the manufacture's protocol. TriReagent RT contains phenol and guanidine thiocyanate in a mono-phase solution to facilitate effective inhibition of RNase activity.

Homogenization

1 ml TriReagent RT was added to $5x10^6$ cells as pellet and subsequently lysed by repetitive pipetting, chemically guanidine thiocyanate enabled this step.

Phase separation

Addition of 4-bromoanisole (BAN) (Molecular Research Center Inc., Cincinnati, USA) and centrifugation (Refrigerated centrifuge SIGMA 3K15, SIGMA GmbH, Osterode am Harz Germany) leads to phase separation: an upper aqueous phase containing RNA, an interphase including DNA and a lower red phenol phase, where proteins remain. This process is facilitated by the second main component phenol, which binds DNA in acidic milieu and subsequently allows the separation of RNA from DNA and proteins. After separation each component can be isolated.

For this step 50 µl of BAN were supplemented and the sample was shaken twenty times. After centrifugation at 12,000 g for 15 minutes at 4°C the three phases became visible.

RNA Precipitation

RNA precipitates from the aqueous phase after addition of isopropanol.

500 µl of the upper aqueous phase were transferred into a fresh tube and mixed with 500 µl of isopropanol (Carl Roth GmbH, Karlsruhe, Germany). After 10 minutes of incubation at room temperature and centrifugation at 12,000 g for 8 minutes at 4°C a small white pellet appeared on the bottom of the tube.

RNA wash

After removement of the supernatant the remaining RNA pellet was washed with 1 ml 75% ethanol and centrifuged at 7500 g for 5 minutes at 4°C. The supernatant was

decanted and the sample was centrifuged at 12000 g for a few seconds. The remains of ethanol were poured off and the pellet was briefly air-dried.

RNA solubilisation

RNase-free water (SIGMA GmbH, Osterode am Harz Germany) was added to the RNA pellet to get it ready for further use or storage. The sample got dissolved for 10 minutes at 55°C at the heating plot. Subsequently, the sample was stored at ice. (51)

Spectroscopic RNA quantification

Analysis of concentration of isolated and purified RNA was performed using the NanoDrop 1000 spectrophotometer (PEQLAB Biotechnology GmbH, Erlangen, Germany). 2 µl of RNase-free water were pipetted to the prescribed measuring point to set a blank. Before each measurement fuzz-free tissue was used to clean the measuring pedestals. Concentration of 2 µl units of the RNA sample was analyzed by the NanoDrop 1000 spectrophotometer as well as the grade of purification.

Subsequently, RNA was diluted to 100 µg/µl with RNase-free water and stored at -20°C.

Electrophoretic RNA quality assessment

To fabricate a 1% agarose gel 0,5 g agarose (Biozym, Vienna, Austria) was mixed to 50 ml 1x TAE (Tris-acetate-EDTA) buffer (Table 1). To dissolve agarose it was heated in a microwave. After cooling down to 50°C, 4 µl ethidium bromide (SIGMA GmbH, Osterode am Harz Germany) was added and the melted agarose solution was poured into the casting tray with the combs. The combs were carefully pulled out as soon as the solution was solid and the solidified agarose gel was put into the electrophoresis unit. The box was filled with TAE buffer until the whole gel was covered.

2 µl of sample RNA, 8 µl nuclease free water and 2 µl loading dye 6x were mixed and pipetted into the wells. The gel ran at 70 V for 40 minutes.

ChemiDoc XRS transilluminator (Bio-Rad Laboratories Ges.m.b.H.,Vienna, Austria) was used to make all separated samples visible and to document the results.

As ethidiumbromid is known as mutagen all working steps were conducted under high safety conditions.

Table 1 – TAE 10x Stock
The stock was diluted 10:1 to make a 1x working solution.

Reagent	Quantity
Tris base	48,4 g
Glacial acetic acid (17,4 M)	11,4 ml
EDTA disodium salt	3,7 g
Deionized water	800 ml
First mixed to dissolve then diluted to 1000 ml, stored ad room temperature.	
Total	**1000 ml**

2.2 Polymerase chain reaction

To analyze the expression of mGluR 1- 8 reverse transcription polymerase chain reaction (RT-PCR) and quantitative polymerase chain reaction (qPCR) were performed. All primer sequences used for PCR amplification of metabotropic glutamate receptors 1- 8 are showen in Table 2 (Invitrogen, Vienna, Austria). Homo sapiens ribosomal protein L30 was used as negative control (Invitrogen, Vienna, Austria).

Table 2 - Primer sequences of metabotropic glutamate receptor 1- 8 (mGluR 1- 8) and L30

Gene symbol	forward primer (F) and reverse primer (R)	product size (bp)	Chromosome
mGluR1	F: GCATGAAGGAGTGCTGAACA R: CGATGTTGCTCCACTCAAGA	275	chr6
mGluR2	F:GGCGGTTCCTACAGTGATGT R: CCTCTAGCTCAAAGGCCTCA	262	chr3
mGluR3	F: CCAGGAGTGAAGTTGGGTGT R: CACGGTCCTGGCAAAGTAAT	315	chr7
mGluR4	F: AACATCCTTCGCCTCTTCAA R: GAGGCCACTGTGGACACATA	179	chr6
mGluR5	F: GTTGTGCCTTCAGATGCTCA R: ACCAACAGCTTCTCGCTGAT	399	chr11
mGluR6	F: CTGTTTGCGATACCCCAGAT R: AGATCTGAACGAAGGCCTCA	214	chr5
mGluR7	F: CGTCAAGCCGGAGAAAGTAG R: ATTCCAGCCTAGGGCCTTTA	226	chr3
mGluR8	F: CCCTGATCTCCTTTCCAACA R: TCACTTAGCTCTGGGGCTGT	288	chr7
L30	F: GAAGTACGTCCTGGGGTACAA R: GTCAGAGTCACCTGGATCAAT	238	

Reverse transcription polymerase chain reaction (RT-PCR)

To perform RT-PCR Qiagen One Step RT-PCR Kit (QIAGEN GmbH, Hilden, Germany) was used. The included QIAGEN OneStep RT-PCR Enzyme Mix contains omniscript and sensiscript reverse transcriptases and hot-start Taq DNA polymerase for amplification. Additionally the kit contains 5x RT-PCR buffer and dNTP Mix.

At first RT-PCR Kit, template RNA, gene-specific primer solutions and nuclease free water were placed on ice for thawing. Then, a master mix was prepared (Table 3), containing all components except the template RNA.

Table 3 - Reaction components for one-step RT-PCR
Qiagen One Step RT-PCR Kit

Component	Volume/reaction
Master mix	
Nuclease free water	10 µl
5x RT-PCR buffer	4 µl
dNTP mix	0,8 µl
Primer forward 30 µM	1,2 µl
Primer reverse 30 µM	1,2 µl
RT-PCR Enzyme Mix	0,8 µl
Template RNA	
Template RNA 100 ng/µl	2 µl
Total volume	**20 µl**

Template RNA was dispended to the PCR tubes, subsequently the appropriate volume of the gently mixed master mix was added. A negative control (without template RNA) and a positive control (with L30 primers) were included. Subsequently, all PCR tubes were placed in the thermal cycler (C100TM Thermal Cycler, Bio-Rad Laboratories Ges.m.b.H.,Vienna, Austria) and the RT-PCR program was started (Table 4). After amplification the samples were stored at -20°C.

Table 4 - Thermal cycler condition for reverse transcription polymerase chain reaction
Performed using the Qiagen One Step RT-PCR Kit

Reverse transcription	30 min	50°C	transcription of cDNA from RNA via reverse transcriptase
Initial PCR activation	15 min	95°C	Activation of hot-start Taq DNA polymerase, Inactivation of reverse transcriptases, denaturation of the cDNA template
3-step cycling			
Denaturation	1 min	94°C	melting of the DNA templates
Annealing	1 min	60°C	Annealing of the primers to the DNA template
Extension	1 min	72°C	Synthesis of a new complementary DNA strand
Number of cycles	38	mGluR1	
	27	L30	
Final extension	10 min	72°C	
Final hold	∞	4°C	Short-term storage

Electrophoretic DNA quality assessment

To analyse RT-PCR products a gel electrophorese was performed. This time a 1,5% agarose gel was prepared (2,25 g agarose, 150 ml 1x TAE buffer and 12 µl ethydium bromide) and placed in the casting tray filled with TAE buffer. For each 20 µl sample 4 µl 6x loading dye were placed in the wells. To measure product size a 100bp ladder standard was used. Additionally, a negative control was added.

Electrophoresis ran for 70 minutes with a voltage of 150 V. To visualize and document all samples the ChemiDoc XRS transilluminator (Bio-Rad Laboratories Ges.m.b.H.,Vienna, Austria) was used.

Quantitative PCR (qPCR)

cDNA synthesis

To synthesize complementary deoxyribonucleic acids (cDNA) from isolated RNA via reverse transcriptase a high capacity RNA to cDNA Kit (Applied Biosystems, Vienna, Austria) was used.

At first a 2x master mix was prepared and placed on ice. All components were mixed gently (Table 5). For one reaction 10 µl of the 2x master mix were transferred to a tube and 10 µl of RNA sample were added. All tubes were briefly centrifuged and loaded into the thermal cycler (C100TM Thermal Cycler, Bio-Rad Laboratories Ges.m.b.H.,Vienna, Austria). Subsequently, the reverse transcription run was started: 10minutes at 25°C, 120 minutes at 37°C for reverse transcription and a 5 second step at 85°C for enzyme inactivation. Generated cDNA (100 ng/µl) was stored at -20°C until further usage.

Table 5 - Reaction components for cDNA synthesis
High capacity RNA to cDNA Kit (Applied Biosystems)

Components	Volume/reaction
Master mix	
10x RT buffer	2 µl
25x dNTP mix	0,8 µl
10x random primers	2 µl
Multiscribe reverse transcriptase	1 µl
Nuclease free water	4,2 µl
Template RNA	
Template RNA 200 ng/µl	10 µl
Total volume per reaction	**20 µl**

Quantitative PCR (qPCR)

For qPCR iQ SybrGreen Supermix (Bio-Rad Laboratories Ges.m.b.H.,Vienna, Austria), a ready-to-use reaction master mix, was used. It contains antibody-mediated hot-start Taq DNA polymerase, all four deoxynucleotides (dNTPs), $MgCl_2$, SYBR®Green I dye, enhancers, stabilizers, and fluorescein.

SybrGreen is a nucleic acid stain which binds to DNA. The DNA-dye-complex emits green light upon excitation, whereby the intensity of the fluorescence depends on the amount of PCR products. This increase of fluorescence allows a quantification of PCR products.

Before performing qPCR the cDNA samples (100 ng/µl) were diluted 1:20 with nuclease free water to 5 ng/µl.

Table 6 - Reaction components for quantitative polymerase chain reaction
iQ SybrGreen Supermix (Bio-Rad Laboratories)

Components	Volume/reaction
iQSybrGreenSupermix	10 µl
Primer forward 0,2 µM	0,4 µl
Primer reverse 0,2 µM	0,4 µl
Nuclease free water	3,2 µl
cDNA (5 ng/µl)	6 µl
Total volume per reaction	**20 µl**

All components were mixed gently and dispersed to a PCR plate (Table 6). CFX96 Real Time PCR Detection System (Bio-Rad Laboratories Ges.m.b.H.,Vienna, Austria) was used for measurement of mGluR expression under the following conditions (Table 7).

Table 7 - Thermal cycler condition for quantitative polymerase chain reaction
Performed using the iQ SybrGreen Supermix (Bio-Rad Laboratories)

Polymerase activation and DNA denaturation	3 min	95°C
3-step cycling		
Denaturation	15 sec	95°C
Annealing	45 sec	60°C
Extension	30 sec	72°C
Number of cycles	50	
Melt curve	every 5 sec	0,5°C increments from 55°C to 95°C

The results were normalized to the reference gene L30. Analysing of the relative gene expression was performed using the ΔΔCq-method by Pfaffl (52).

3. Chemicals

3.1 mGluR1 antagonists

Cyclothiazide (CTZ) (Tocris Bioscience, R&D Systems Company) was solved in dimethylsulfoxid (DMSO) to 40 mM. YM 298198 hydrochloride (Tocris Bioscience, R&D Systems Company) was dissolved in aqua bidest (A.D.) to 20 mM. Both mGluR1 antagonists were stored at -20°C until usage.

For experiments cells were treated with increasing concentrations (10 µM, 50 µM, 100 µM and 200 µM) of both abovementioned mGluR1 antagonists.

3.2 Temozolomide

The DNA methylating, chemotherapeutic agent Temozolomide (TZM) (Tocris Bioscience, R&D Systems Company) was dissolved in DMSO to 80 mM and stored at -20°C.

For experiments treatment with 200 µM TZM was combined with different concentrations (100 µM and 200 µM) of mGluR1 antagonists and compared to treatment with each substance alone.

4. Cultivation and experimental protocol

All aforementioned cell lines were cultivated in Ham's F12:M199 (PAA, Pasching, Austria) 1:1 with 10% foetal bovine serum (FBS) (Biochrom, Tutzing, Germany) using vented cap cell culture flasks (Sarstedt, Wiener Neudorf, Austria) at 37°C, 5% CO_2 and 95% humidity (Heraeus Instruments, Langenselbold, Germany) with a starting concentration of $2x10^5$ cells/ ml. After three or four days, depending on the growth rate, new medium was added or cells were subcultured to the starting concentration. All experiments were performed without the usage of antibiotics and under sterile conditions (Hera Safe, Heraeus Instruments, Germany).

For experiments 20 ml cell suspension was transferred from the culture flask to a centrifugal tube (Sarstedt, Wiener Neudorf, Austria). After centrifugation at 1,000 g for five minutes (GS-6 centrifuge, Beckman, USA) the supernatant was removed. Subsequently, the remaining cell pellet was resuspended in 20 ml growth medium by gentle mixing with the pipette. After cell counting the cell suspension was diluted to

$2x10^5$ cells/ ml and 4 ml samples were transferred to a 6 well plate (Sarstedt, Wiener Neudorf, Austria). Then, different concentration of the mGluR1 antagonists and TZM were added to individual wells. DMSO was used as negative control for CTZ treated cells and A.D. for YM treated cells. Hereafter, three subsamples (1,2 ml) of each 4 ml sample were transferred to a 24 well plate (Sarstedt, Wiener Neudorf, Austria). After 24, 48 or 72 h of incubation, light microscopy, cell counting and analysing of the metabolic cell activity with the WST-1 assay were performed.

5. Microscopy

Light microscopy was performed before, during and after all experiments to observe morphological changes (Nikon Eclipse TE300, Melville, USA). Pictures were taken for documentation (Nikon Digital Sight DS-L1, Melville, USA).

6. Cell Counting and Analysing – Casy-1® Cell Counter

Measurement of cell counts and cell size was performed by electronic cell counter CASY-1® Cell Counter & Analyser TT (Schärfe Systems, Reutlingen, Germany). The cursor was set to 7.5 µm as the threshold for dead cells/ debris and 30 µm as the threshold for cell clusters. To disperse cell aggregates of the sample into single cells the suspension was resuspended carefully. Then 50 µl of the cell suspension were added to 10 ml Casy®Ton isotonic dilution liquid (Roche, Wien, Austria). For each sample four aliquots of this 1:200 dilution were analysed. The program calculated the total number of cells per ml and the mean diameter.

7. WST-1 assay

The Cell Proliferation Reagent water-soluble tetrazolium salt 1 (WST-1) (Roche Diagnostics, Mannheim, Germany), a clear, slightly red, ready-to-use solution, was used for the non-radioactive, spectrophotometric quantification of cell viability. The assay is based on the enzymatic cleavage of the tetrazolium salt WST-1 to formazan, which is dark red. A higher number of viable cells lead to an increased activity of the mitochondrial dehydrogenase in the cell sample. Therefore, the number of metabolic active cells correlates with the amount of formazan dye. For quantification of the formazan dye a microplate (ELISA) reader is necessary.

After cells were carefully suspended to single cells, from each sample six subsamples (100 µl) were transferred to a 96-well microplate (Sarstedt INC., Newton, USA). 10 µl Cell Proliferation Reagent WST-1 was added to each well. Additionally, 100 µl culture medium and 10 µl Cell Proliferation Reagent WST-1 were added into six wells as a blank for the ELISA reader. After two hours of incubation, the plate was shaken for one minute (MS1 Minishaker, IKA-Werke GmbH & Co. KG, Staufen, Germany). Then, the measurement of the absorbance of the samples against the background control as blank was performed using a microplate (ELISA) reader (Thermomax Microplate Reader, Molecular Devices, Biberach an der Riss, Germany) at 450 nm. As reference wavelength 650 nm was chosen.

8. Statistical Analysis

Statistical analysis was performed using the Student's t-test, whereby $p < 0.05$ was considered significant (*) and $p < 0.01$ highly significant (**).

C. RESULTS

1. Expression of mGluR1 in NET cell lines

Amplified RT-PCR products were analysed using an electrophoretic DNA quality assessment. Two 100 bp standards, one on the left and one on the right, surround the eight NET samples, including four MTC (MTC-SK, SHER-I, RARE and BOJO (53)) and four SI-NET (KRJ-I, P-STS, L-STS and H-STS) samples. On the right side, water (A.D.) is representing the negative control. Fig. 8 shows results for mGluR1. All NET samples display bands of variable intensities and a product size close to 300 bp. These results match to the expected product size of 275 bp. RARE and H-STS samples show additional bands. Negative control did not show a signal.

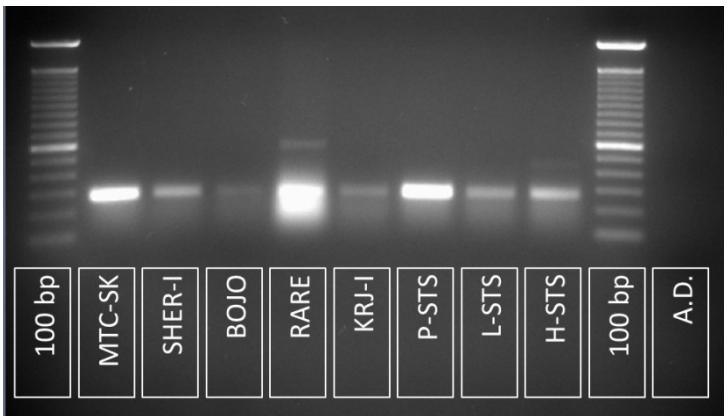

Fig. 8 - Gel electrophoresis for mGluR1 products

In Fig. 9 the results for L30 as the positive control are shown. All eight bands appear in similar intensity, consistent with the expected size of 238 bp. Water as the negative control showed no signal.

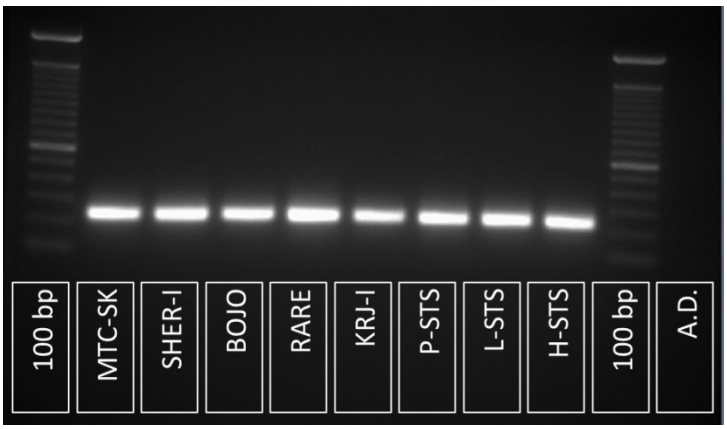

Fig. 9 - Gel electrophoresis for L30 products.

Quantitative real-time PCR was performed on MTC-SK, KRJ-I, P-STS, L-STS and HF-SAR cell lines. HF-SAR cells are normal human skin fibroblasts (personal communication R. Pfragner). Fig. 10 shows relative gene expression analysed by normalization of expression levels to the transcriptional level of mGluR1 - 8 on HF-SAR cells.

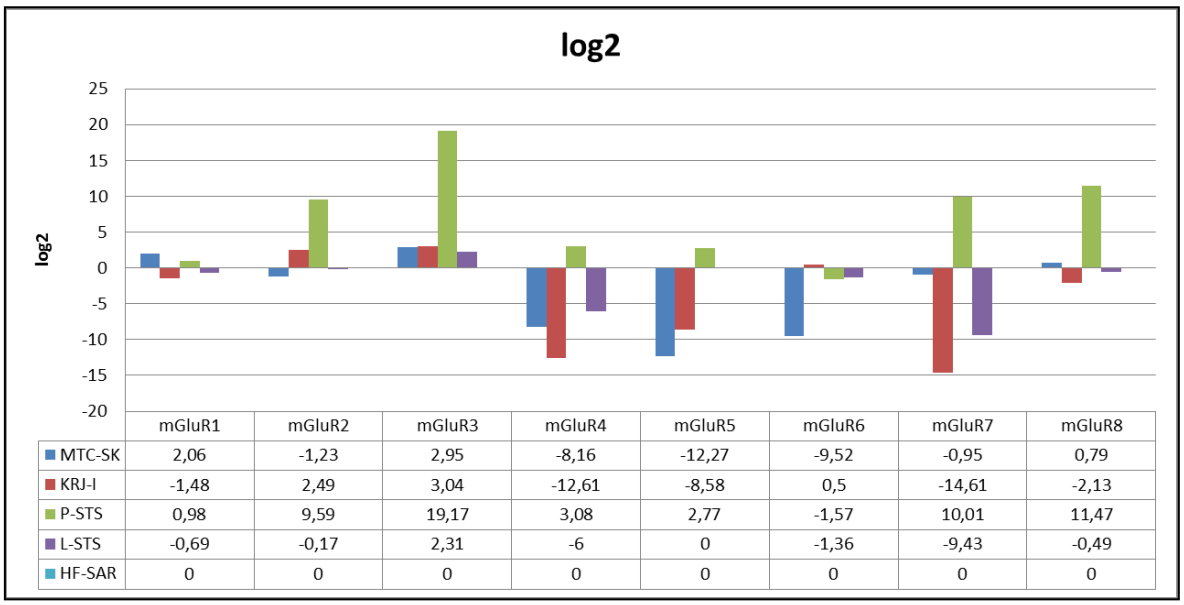

	mGluR1	mGluR2	mGluR3	mGluR4	mGluR5	mGluR6	mGluR7	mGluR8
MTC-SK	2,06	-1,23	2,95	-8,16	-12,27	-9,52	-0,95	0,79
KRJ-I	-1,48	2,49	3,04	-12,61	-8,58	0,5	-14,61	-2,13
P-STS	0,98	9,59	19,17	3,08	2,77	-1,57	10,01	11,47
L-STS	-0,69	-0,17	2,31	-6	0	-1,36	-9,43	-0,49
HF-SAR	0	0	0	0	0	0	0	0

Fig. 10 - Relative gene expression of mGluR1 – 8 on several NET cell lines
Results are compared to the transcriptional level on HF-SAR cells.

2. Morphology

All NET cell lines except of P-STS cell line form spheroid cell aggregations.

2.1 SI-NET cell lines

It was not possible to observe morphological changes in P-STS cells, which appear in slackly monolayer, after treatment with mGluR1 antagonists.

CTZ reduced the diameter of the spheroid cell aggregates in KRJ-I. YM led to a dissociation of the spheroid cell formations in KRJ-I and H-STS cells (Fig. 11). Combination of TZM with YM led, like YM alone, to a dissociation of cell clusters in KRJ-I and H-STS cells, whereby TZM alone did not cause morphological changes of cell spheroids.

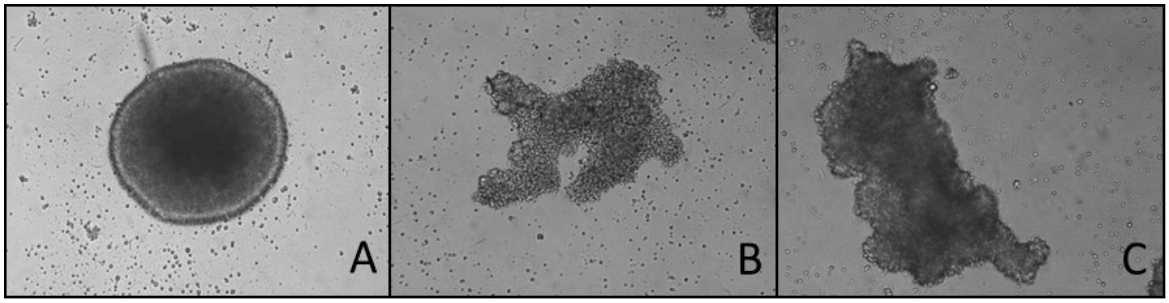

Fig. 11 - Morphological changes observed by light microscopy in KRJ-I cells (Magnification of 100 times)
A: Spheroid cell formation of the A.D. control; B: Dissociation of cell clusters after treatment with YM; C: Dissociation of cell clusters after treatment with YM and TZM

2.2 MTC cell lines

CTZ treated MTC-SK cells appeared in smaller spheroid cell aggregates, YM led to a dissociation of cell clusters (Fig. 12). No morphological changes of SHER-I cells concerning cell formation were detectable.

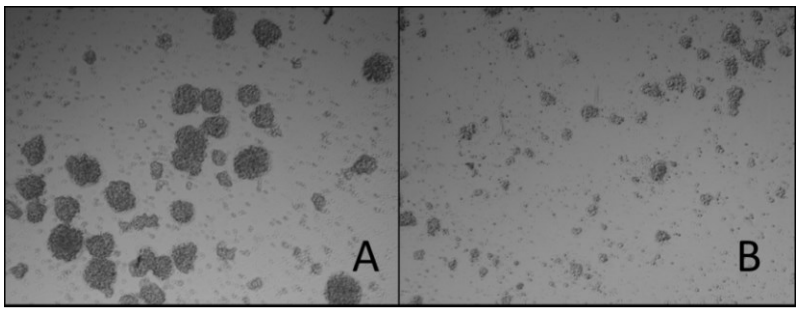

Fig. 12 - Morphological changes observed in MTC-SK cells
(Magnification of 40 times)
A: Spheroid cell clusters of MTC-SK cells after treatment with DMSO as negative control
B: Smaller cell aggregates after treatment with 200 µM CTZ

3. Proliferation

3.1 SI-NET cell lines

Single treatment with mGluR1 antagonists

CTZ led to a dose-dependent inhibition of proliferation in all SI-NET cell lines compared to the cells treated with DMSO as negative control (Table 8). 200 µM CTZ caused a highly significant reduction of cell counts in KRJ-I (Fig. 13), P-STS (Fig. 15) and H-STS cells. Same concentration led to a significant inhibition of proliferation in L-STS cells.

Table 8 – Effects of different concentrations of CTZ on proliferation of SI-NET cell lines
Proliferation of KRJ-I, P-STS, L-STS and H-STS cells relatively compared to DMSO control (100%)

	KRJ-I		P-STS		L-STS		H-STS	
DMSO control	100%		100%		100%		100%	
10 µM CTZ	91,43%	*	92,09%	*	102,21%		94,94%	*
50 µM CTZ	82,09%	**	91,16%	**	93,99%		88,55%	*
100 µM CTZ	67,21%	*	85,23%	**	79,48%	*	74,72%	**
200 µM CTZ	57,80%	**	80,49%	**	58,49%	*	61,03%	**

Three days treatment with YM had different effects on proliferation of SI-NETs (Table 9, Fig. 16). Treatment with 200µM and 100µM YM led to inhibition of proliferation in a dose dependent manner. In some experiments, lower concentrations of YM caused increasing cell counts compared to cells treated with A.D. as negative control.

Table 9 – Effects of different concentrations of YM on proliferation of SI-NET cell lines
Proliferation of P-STS, L-STS and H-STS cells relatively compared to A.D. control (100%)

	P-STS		L-STS		H-STS	
A.D. control	100%		100%		100%	
10 µM YM	92,38%	*	103,42%	*	120,53%	
50 µM YM	90,01%	*	94,56%		116,30%	
100 µM YM	80,51%	**	89,98%	**	95,81%	
200 µM YM	72,66%	**	65,49%	**	57,98%	**

YM showed various effects on proliferation of KRJ-I cells dependent on the passage numbers (Table 10). 200 µM YM caused a stronger reduction of cell counts in lower passages of KRJ-I cells than in higher passages. In some experiments, lower concentrations led to an increase of cell counts in higher passages of KRJ-I cells (Fig. 14).

Table 10 - Effects of different concentrations of YM on proliferation of KRJ-I cells
Proliferation of higher and lower passages of KRJ-I cells relatively compared to A.D. control (100%)

	KRJ-I higher passage		KRJ-I lower passages	
A.D. control	100%		100%	
10 µM YM	126,22%	**	105,99%	
50 µM YM	116,12%	**	99,70%	
100 µM YM	104,59%		88,18%	
200 µM YM	78,81%	*	63,83%	*

Cell proliferation SI-NETs – single treatment

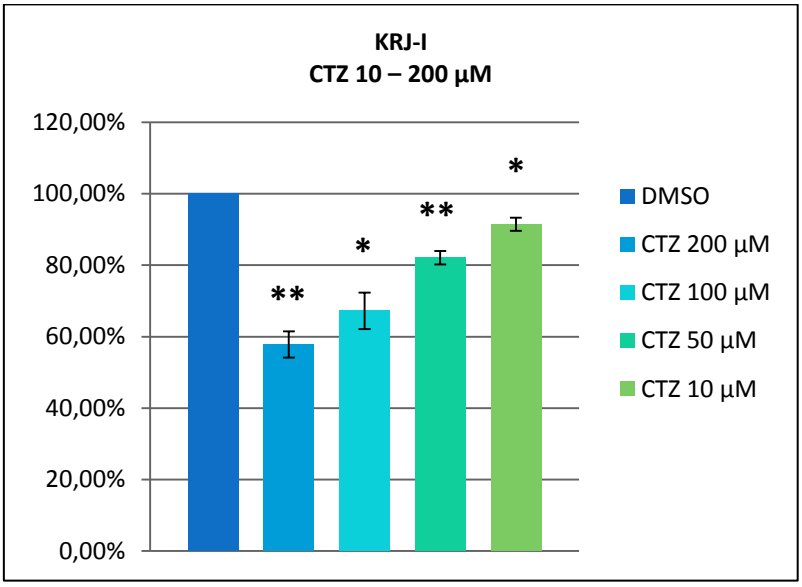

Fig. 13 – Proliferation of KRJ-I cells after single treatment with CTZ
The mGluR1 antagonist CTZ inhibited proliferation of KRJ-I cells in a dose dependent manner compared to DMSO as negative control.

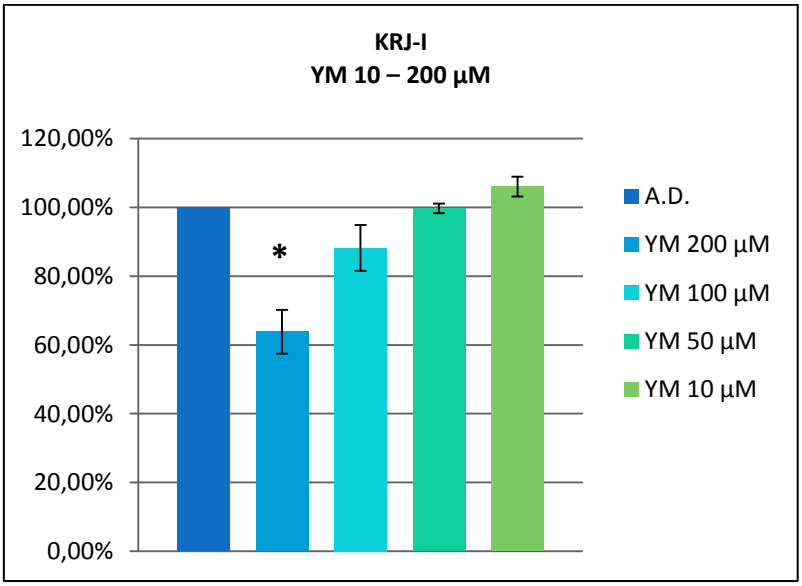

Fig. 14 – Proliferation of KRJ-I cells after single treatment with YM
The mGluR1 antagonist YM inhibited proliferation of KRJ-I cells in a dose dependent manner compared to A.D. as negative control.

Cell proliferation SI-NETs – single treatment

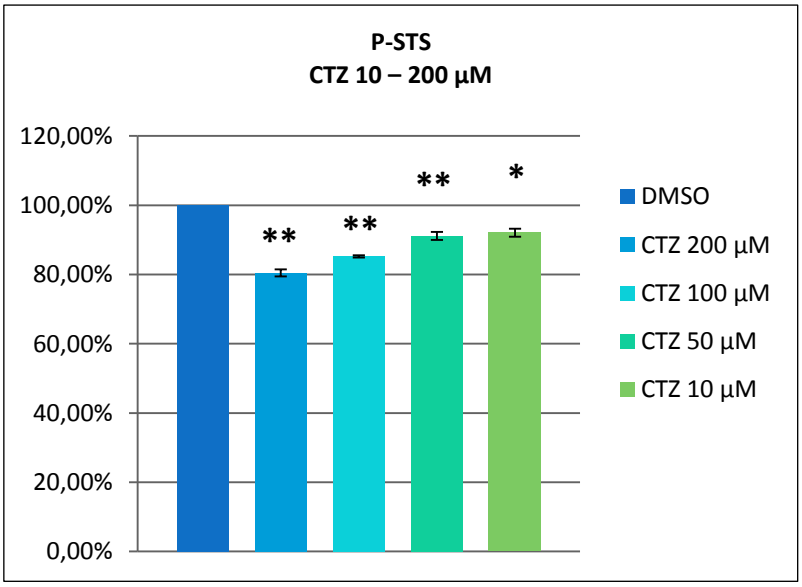

Fig. 15 – Proliferation of P-STS cells after single treatment with CTZ
The mGluR1 antagonist CTZ inhibited proliferation of P-STS cells in a dose dependent manner compared to DMSO as negative control.

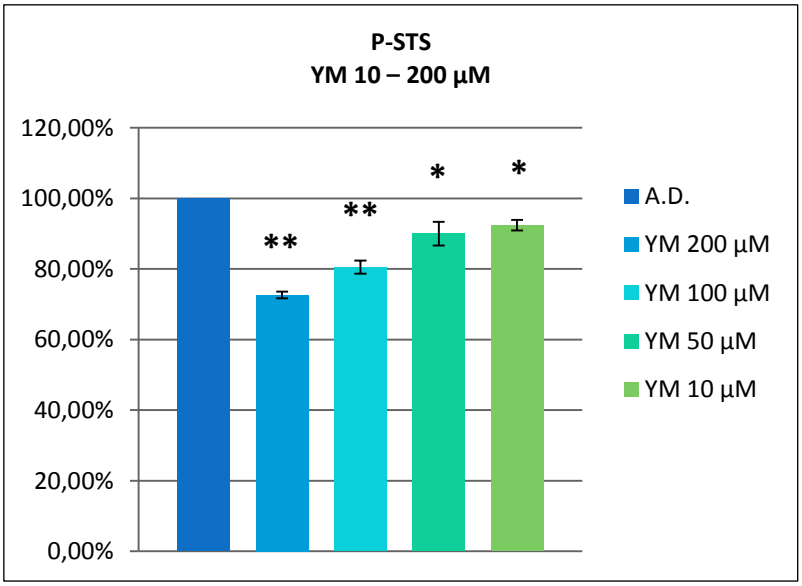

Fig. 16 – Proliferation of P-STS cells after single treatment with YM
The mGluR1 antagonist YM inhibited proliferation of P-STS cells in a dose dependent manner compared to A.D. as negative control.

Combined treatment with the mGluR1 antagonists (CTZ and YM) and the chemotherapeutic agent TZM

Treatment with TZM (200 µM) alone led to highly significant reduction of cell growth in KRJ-I. Combination of YM (200 µM) and TZM (200 µM) caused a stronger inhibition of proliferation than single treatment (Fig. 18), but combined therapy with CTZ (200 µM or 100µM) and TZM (200 µM) did not cause a similar effect (Fig. 19).

In some experiments, treatment with TZM (200 µM) decreased cell counts of P-STS cells. Combined treatment with CTZ (200 µM) and TZM (200 µM) caused a stronger reduction of cell counts than single treatment with CTZ or TZM (Fig. 20). Combination of YM and TZM did not show a similar synergistic effect (Fig. 21).

Cell proliferation SI-NETs – combined therapy

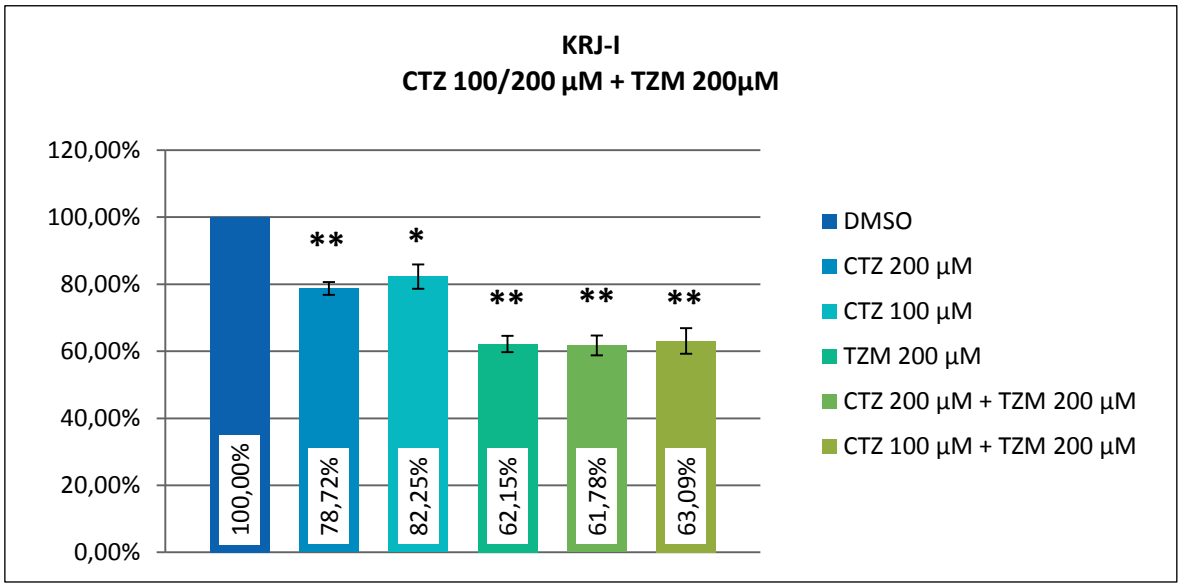

Fig. 17 – Proliferation of KRJ-I cells after combined treatment with CTZ and TZM
Combination of CTZ and TZM caused a slightly stronger inhibition of proliferation than single treatment. TZM alone led to a highly significant inhibition of cell growth.

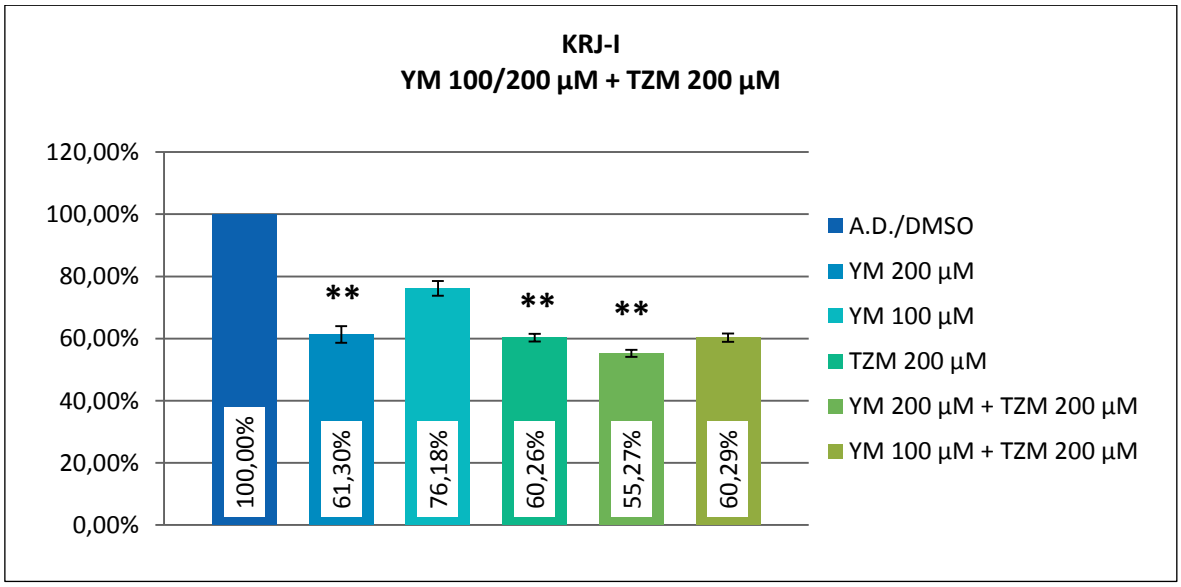

Fig. 18 – Proliferation of KRJ-I cells after combined treatment with YM and TZM
Combination of YM (200 µM) and TZM (200 µM) caused a stronger inhibition of proliferation than single treatment. TZM led to a highly significant inhibition of cell growth.

Cell proliferation SI-NETs – combined treatment

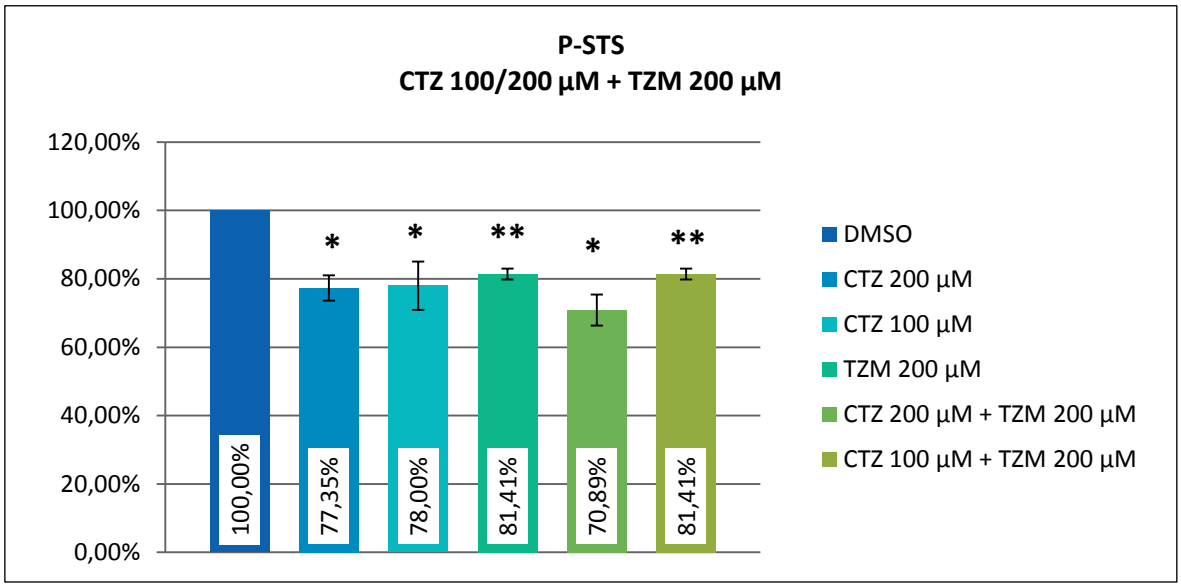

Fig. 19 – Proliferation of P-STS cells after combined treatment with CTZ and TZM
TZM led to a highly significant inhibition of proliferation. Combination of the mGluR1 antagonist CTZ (200 µM) caused stronger inhibition of cell growth than single treatment. Results refer to a single experiment.

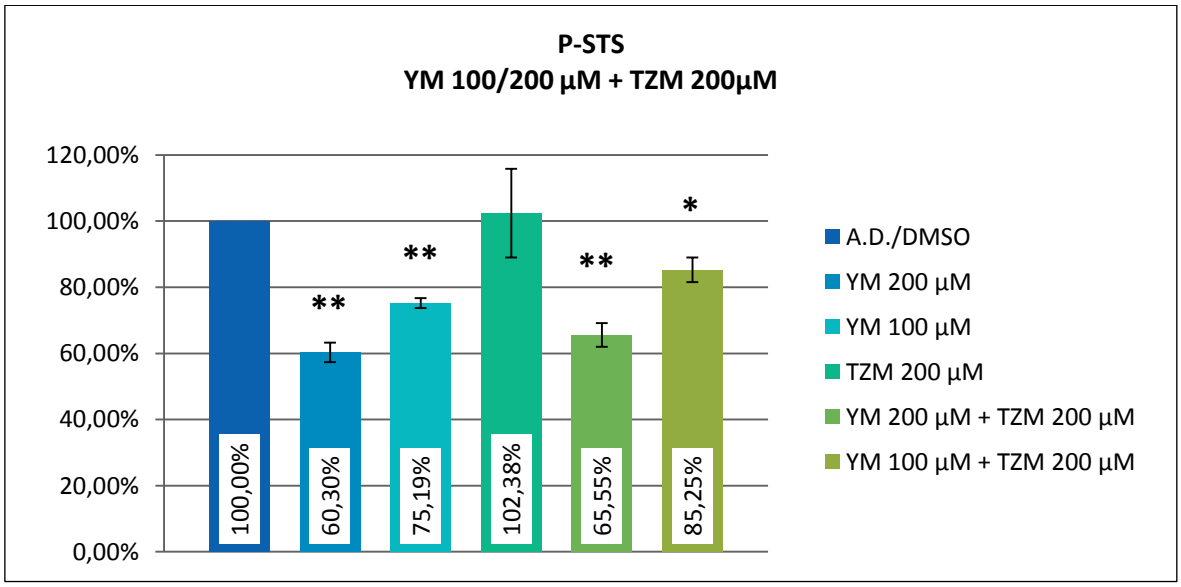

Fig. 20 – Proliferation of P-STS cells after combined treatment with YM and TZM
Combination of mGluR1 antagonist YM (200 µM) caused stronger inhibition of cell growth than single treatment with TZM. TZM did not cause an inhibition of proliferation.

3.2 MTC cell lines

Single treatment with mGluR1 antagonists

CTZ inhibited the growth of MTC cells (MTC-SK and SHER-I) in a dose dependant manner, whereby the dosage of 200 µM was the most effective and led to a highly significant reduction of cell counts in MTC-SK (Fig. 21) and in SHER-I (Fig. 23) cells (Table 11).

Table 11 - Effects of different concentrations of CTZ on proliferation of MTC cell lines
Proliferation of MTC-SK and SHER-I cells relatively compared to DMSO control (100%).

	MTC-SK		SHER-I	
DMSO control	100%		100%	
10µl CTZ	99,22%		95,84%	
50µl CTZ	91,26%		86,79%	**
100µl CTZ	75,10%	*	72,32%	**
200µl CTZ	61,81%	**	56,76%	**

YM treatment (200µM and 100µM) led to a reduction of cell growth in MTC cell lines (Fig. 22 and 24), whereby the dosage of 200 µM had high significant and significant effects on proliferation (Table 12). Again in some experiments, dosage of 10 µM led to a slight increase of cell counts in both tumor cell lines.

Table 12 – Effects of different concentrations of YM on proliferation of MTC cell lines
Proliferation of MTC-SK and SHER-I cells relatively compared to A.D. control (100%)

	MTC-SK		SHER-I	
A.D. control	100%		100%	
10 µl YM	102,41%		104,65%	
50 µl YM	91,69%		100,17%	
100 µl YM	85,26%	*	92,08%	
200 µl YM	68,47%	**	64,84%	*

Cell proliferation MTCs – single treatment

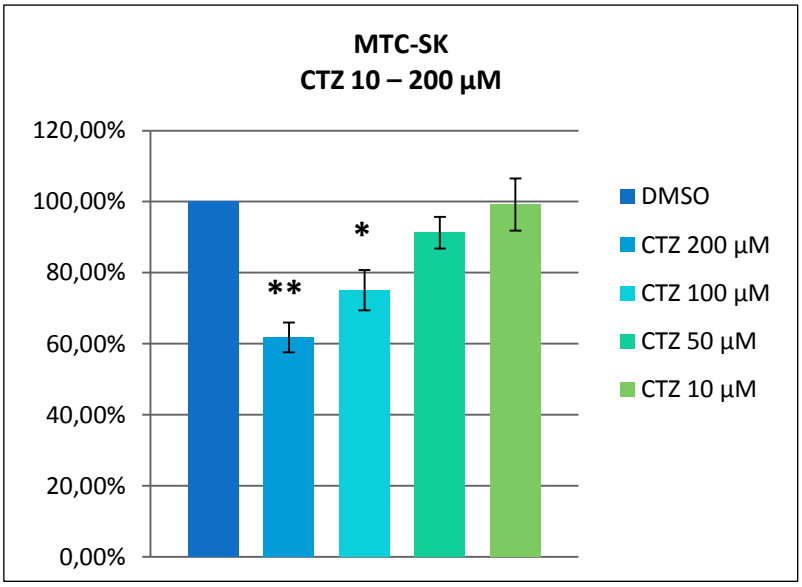

Fig. 21 - Proliferation of MTC-SK cells after single treatment with CTZ
The mGluR1 antagonist CTZ inhibited proliferation of MTC-SK cells in a dose dependent manner compared to DMSO as negative control.

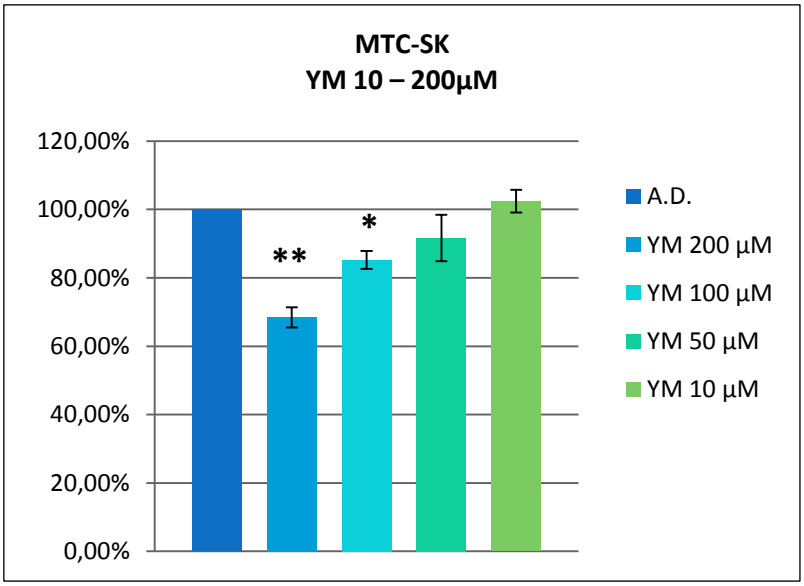

Fig. 22 - Proliferation of MTC-SK cells after single treatment with YM
The mGluR1 antagonist YM inhibited proliferation of MTC-SK cells in a dose dependent manner compared to A.D. as negative control.

Cell proliferation MTCs – single treatment

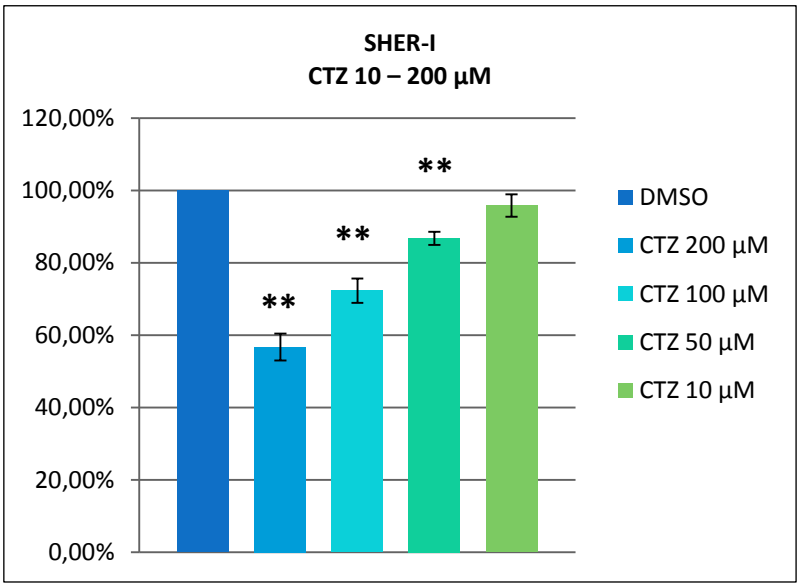

Fig. 23 - Proliferation of SHER-I cells after single treatment with CTZ
The mGluR1 antagonist CTZ inhibited proliferation of SHER-I cells in a dose dependent manner compared to DMSO as negative control.

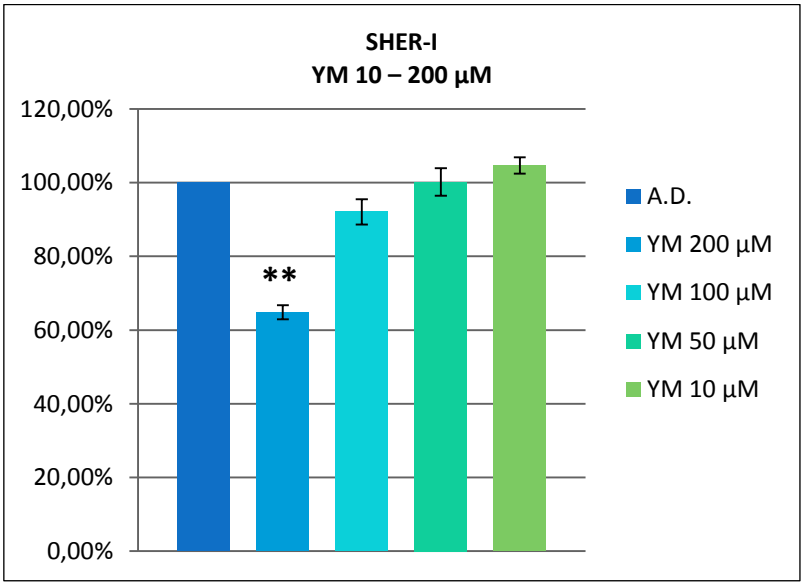

Fig. 24 - Proliferation of SHER-I cells after single treatment with YM
The mGluR1 antagonist YM inhibited proliferation of SHER-I cells in a dose dependent manner compared to A.D. as negative control.

Combined treatment with the mGluR1 antagonists (CTZ and YM) and the chemotherapeutic agent TZM

TZM (200 µM) led to a highly significant reduction of cell counts in MTC-SK cells. Combined treatment with CTZ or YM (200 µM) and TZM (200 µM) induced a stronger inhibition of proliferation of MTC-SK cells than single treatment. Similar synergistic effects were reported after combined treatment at a dosage of 100 µM (Fig. 25 and 26).

TZM (200 µM) caused inhibition of proliferation in SHER-I cells. Combined treatment with the mGluR1 antagonist CTZ (200 µM and 100 µM) and TZM (200 µM) induced a slightly stronger inhibition of proliferation in SHER-I cells than single treatment. Combination of YM (200 µM) and TZM did not cause a synergistic inhibition of cell growth, but combined treatment with YM (100 µM) and TZM (Fig. 27 and 28).

Cell proliferation MTCs – combined treatment

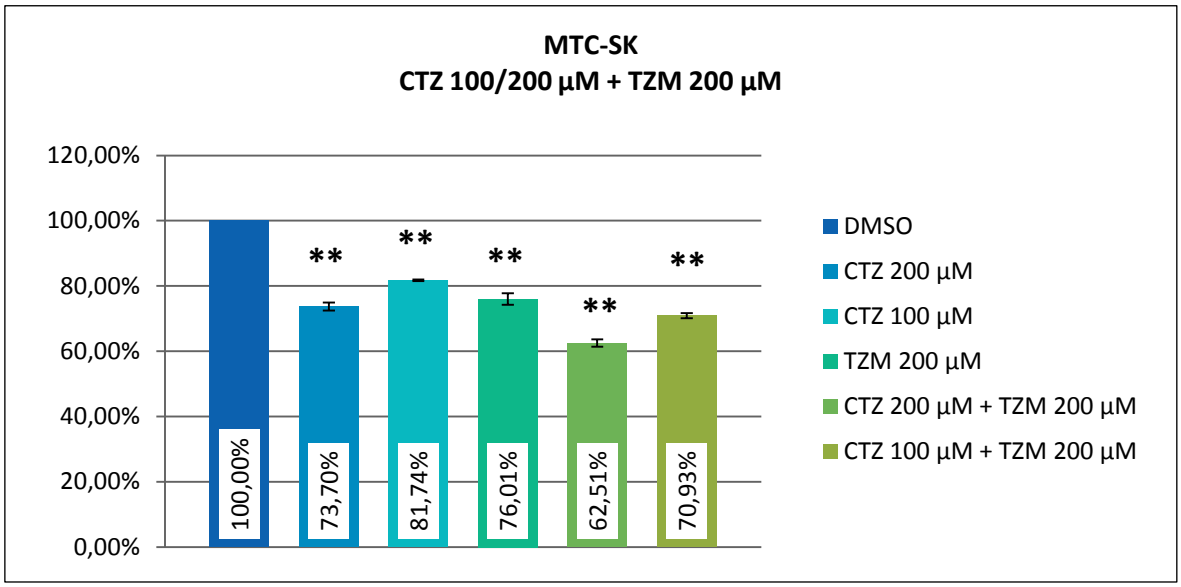

Fig. 25 – Proliferation of MTC-SK cells after combined treatment with CTZ and TZM
Combination of CTZ and TZM caused a stronger inhibition of proliferation than single treatment. TZM alone led to a highly significant inhibition of cell growth.

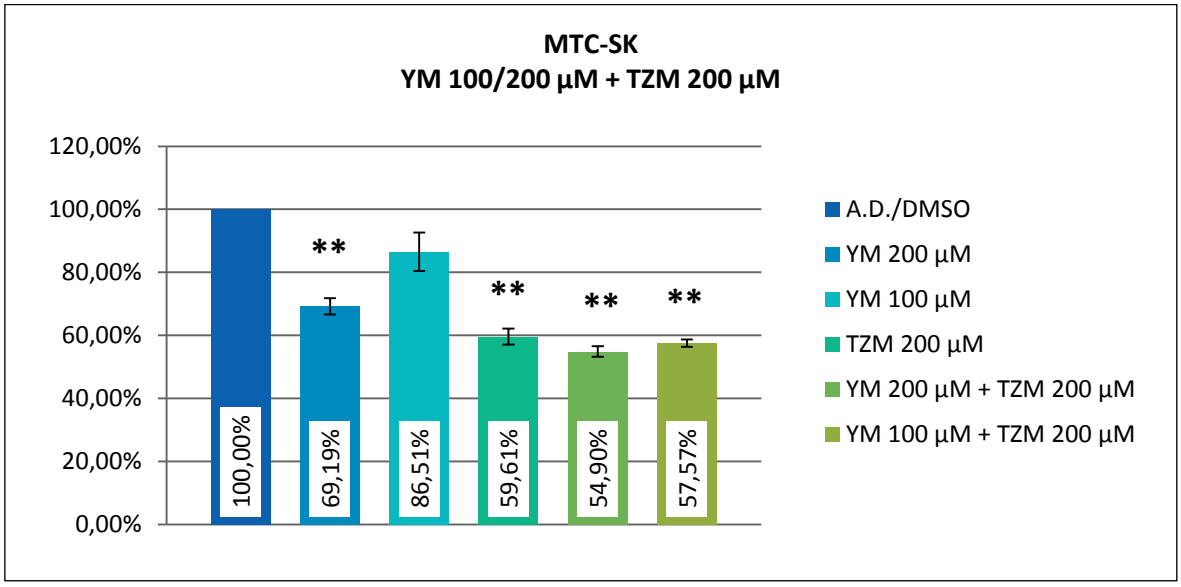

Fig. 26 – Proliferation of MTC-SK cells after combined treatment with YM and TZM
Combination of YM and TZM caused a stronger inhibition of proliferation than single treatment. TZM led to a highly significant inhibition of cell growth.

Cell proliferation MTCs – combined treatment

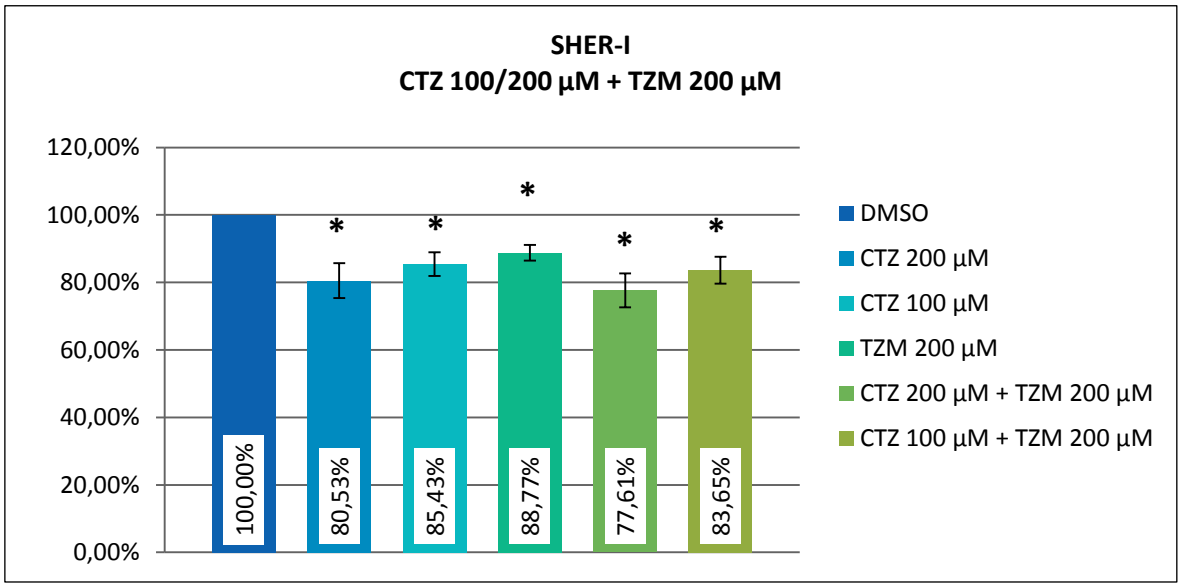

Fig. 27 – Proliferation of SHER-I cells after combined treatment with CTZ and TZM
Combination of CTZ and TZM caused a slightly stronger inhibition of proliferation than single treatment. TZM alone led to a significant inhibition of cell growth.

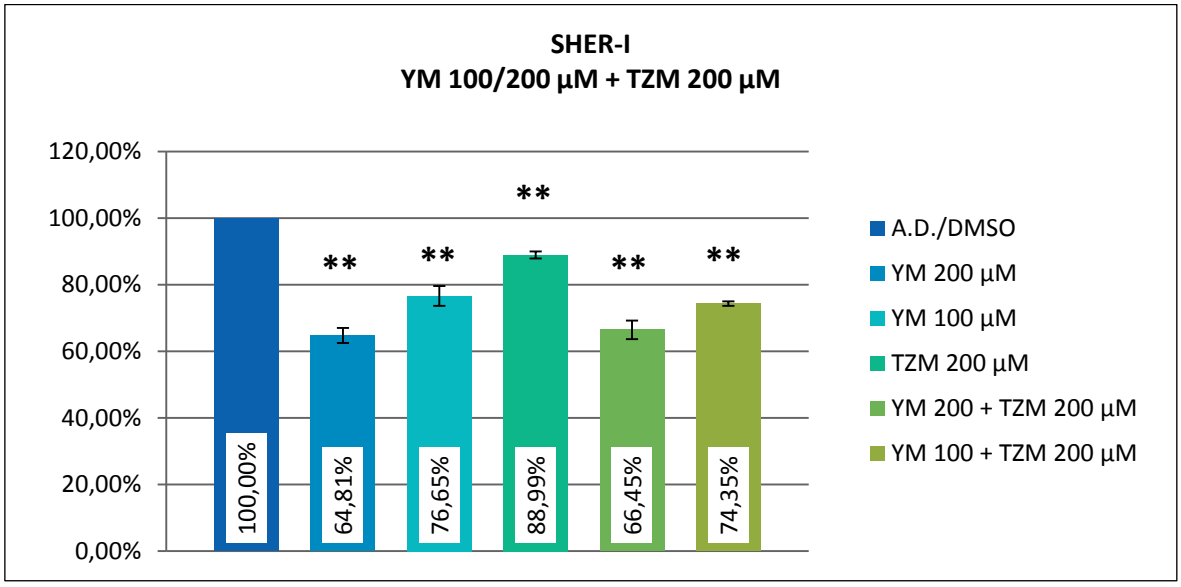

Fig. 28 – Proliferation of SHER-I cells after combined treatment with YM and TZM
Combination of YM (100 µM) and TZM (200 µM) caused a stronger inhibition of proliferation than single treatment. TZM led to a highly significant inhibition of cell growth.

4. Cell size

4.1 SI-NET cell lines

Single treatment with mGluR1 antagonists

Treatment with mGluR1 antagonists (CTZ and YM) had effects not only on cell counts, but also on cell size of SI-NET cells (Table 13).

CTZ (100 µM and 200 µM) led to a reduction of the mean diameter in KRJ-I, L-STS and H-STS cells compared to DMSO. YM (200 µM) caused a similar effect like CTZ on cell size of KRJ-I, L-STS and H-STS cells compared to A.D. as negative control. Both mGluR1 antagonists increased cell size of P-STS cells.

Table 13 – Effects of the mGluR1 antagonists on cell size of SI-NET cells
Influence of the mGluR1 antagonists (CTZ or YM) on the mean diameter of KRJ-I, P-STS, L-STS and H-STS cells. Three days treatment led to an increase (↑) or decrease (↓) of cell size.

	KRJ-I	P-STS	L-STS	H-STS
CTZ 200 µM	↓	↑	↓ *	↓ *
CTZ 100 µM	↓ *	↑ *	↓	↓ *
YM 200 µM	↓ *	↑	↓	↓ *
YM 100 µM	↑	↑ *	↑ *	↓

Combined treatment with mGluR1 antagonists (CTZ and YM) and the chemotherapeutic agent TZM

TZM (200 µM) caused a highly significant increase of the mean diameter of KRJ-I cells. Combined therapy with the mGluR1 antagonists (CTZ and YM) and TZM led to a smaller cell size compared to single treatment with TZM.

Treatment with TZM showed also a significant increase of the mean diameter in P-STS cells compared to DMSO treated cells. Combined treatment with the mGluR1 antagonists (CTZ and YM) and TZM led to larger cell size compared to the negative control.

4.2 MTC cell lines

Single treatment with mGluR1 antagonists

Single treatment with CTZ (100 and 200 µM) and YM (100 and 200 µM) significantly decreased the cell size of MTC-SK cells (Table 14). In contrast, CTZ (100-200 µM) did not significantly influence the cell size of SHER-I cells, even though there is a trend towards a decrease of cell size. Single treatment with YM (100 µM) caused a significant increase of the mean diameter of SHER-I cells compared to A.D. as negative control.

Table 14 – Effects of the mGluR1 antagonists on cell size of MTC cells
Influence of the mGluR1 antagonists (CTZ or YM) on the mean diameter of MTC-SK and SHER-I cells. Three days treatment led to an increase (↑) or decrease (↓) of cell size.

	MTC-SK	SHER-I
CTZ 200 µM	↓ *	↓
CTZ 100 µM	↓ *	↓
YM 200 µM	↓ **	↑
YM 100 µM	↓ *	↑ **

Combined treatment with the mGluR1 antagonists (CTZ and YM) and the chemotherapeutic agent TZM

TZM (200 µM) caused an increase of the mean diameter of MTC-SK cells. Combined therapy with the mGluR1 antagonists and TZM showed smaller cell size than single treatment with TZM, even though these results did not reach statistical significance.

Single therapy with TZM led to a significant increase of cell size of SHER-I cells compared to the negative control. Combined treatment with the mGluR1 antagonists (100 µM and 200 µM) and TZM reduced the mean diameter.

5. WST-1 assay

5.1 SI-NET cell lines

Single treatment with mGluR1 antagonists

Treatment with the mGluR1 antagonists CTZ or YM alone (100 and 200 µM) led to a decrease of mitochondrial activity in KRJ-I cells in a dose dependent manner, whereby the dosage of 200 µM was the most effective (Table 15). YM caused stronger reduction of mitochondrial activity in KRJ-I cells of a lower passage. Both mGluR1 antagonists (200 µM) showed the strongest inhibition of the mitochondrial dehydrogenase at the third day of incubation (Fig. 29 and 30).

Table 15 – Effects of the mGluR1 antagonists on mitochondrial activity of KRJ-I cells
Mitochondrial activity of KRJ-I cells after single treatment with CTZ and YM (200 µM) analysed by the WST-1 assay compared to a negative control (100%)

KRJ-I	CTZ 200µM		YM 200µM (lower passage)		YM 200µM (higher passage)	
day 1	56,48%	**	50,33%	*	71,99%	**
day 2	50,66%	*	40,42%	*	67,43%	*
day 3	45,06%	*	39,19%	*	55,67%	*

Single treatment with the mGluR1 antagonists also led to a dose-dependent inhibition of mitochondrial activity of other SI-NET cell lines (P-STS, L-STS and H-STS) (Table 16 and 17). CTZ and YM reduced the amount of metabolic active cells compared to the negative control in a high significant or significant way, dependent on dosage and cell line.

Table 16 – Effects of CTZ on mitochondrial activity of SI-NET cell lines
Mitochondrial activity of P-STS, L-STS and H-STS cells after treatment with the mGluR1 antagonist CTZ (100 and 200 µM) analysed by the WST-1 assay, compared to DMSO as negative control (100%)

		CTZ 200 µM		CTZ 100 µM	
P-STS	**day 1**	81,27%	**	86,11%	*
	day 2	79,67%	*	90,21%	
	day 3	76,15%	**	83,91%	*
L-STS	**day 1**	42,94%	**	64,81%	*
	day 2	38,42%	**	62,30%	**
	day 3	44,21%	**	66,23%	**
H-STS	**day 1**	34,02%	**	46,22%	**
	day 2	34,90%	**	48,63%	**
	day 3	51,04%	*	63,61%	*

Table 17 – Effects of YM on mitochondrial activity of SI-NET cell lines
Mitochondrial activity of P-STS, L-STS and H-STS cells after treatment with the mGluR1 antagonist YM (100 and 200 µM) analysed by the WST-1 assay, compared to A.D. as negative control (100%)

		YM 200 µM		YM 100 µM	
P-STS	**day 1**	70,41%	**	85,67%	**
	day 2	53,45%	**	74,73%	**
	day 3	44,23%	**	75,44%	*
L-STS	**day 1**	62,74%	*	91,86%	*
	day 2	44,65%	*	83,88%	*
	day 3	36,60%	*	83,89%	*
H-STS	**day 1**	14,85%	**	49,93%	**
	day 2	7,70%	**	53,36%	**
	day 3	8,66%	**	79,67%	

Mitochondrial activity SI-NETs – single treatment

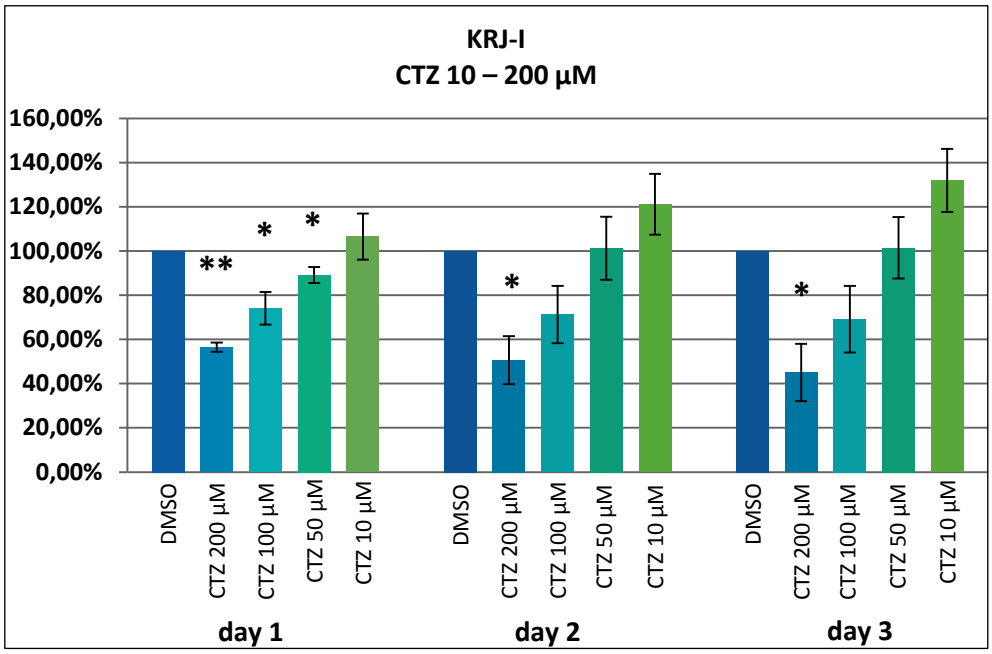

Fig. 29 – Mitochondrial activity of KRJ-I cells after single treatment with CTZ
Mitochondrial activity of KRJ-I cells after single treatment with CTZ analysed by the WST-1 assay compared to a negative control (100%). Similar effects were obtained in experiments with P-STS cells.

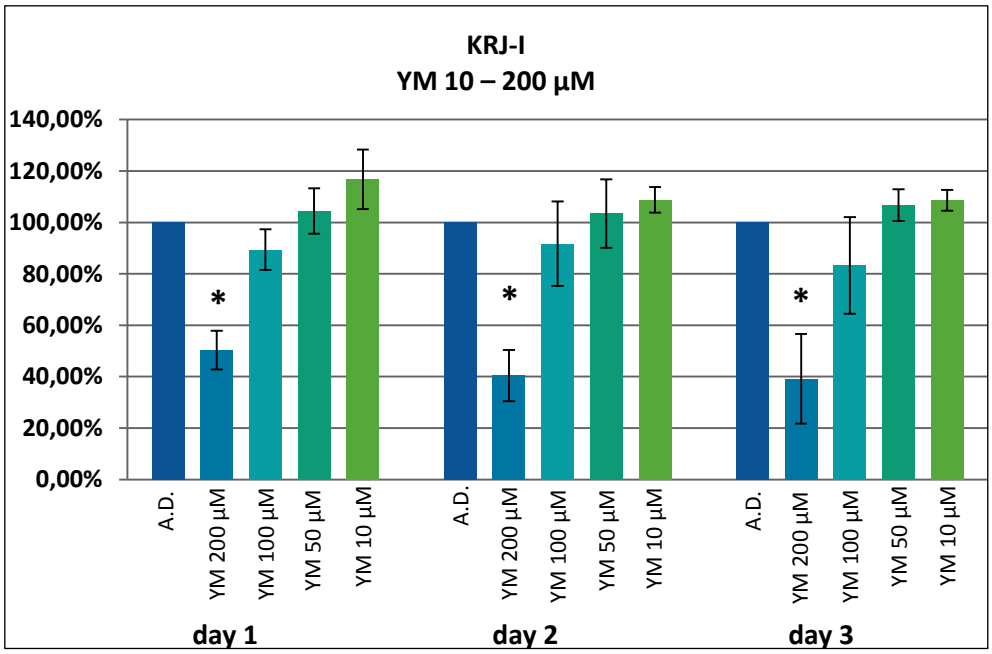

Fig. 30 – Mitochondrial activity of KRJ-I cells after single treatment with YM
Mitochondrial activity of KRJ-I cells (lower passage) after single treatment with YM analysed by the WST-1 assay compared to a negative control (100%). Similar effects were obtained in experiments with P-STS cells.

Combined treatment with the mGluR1 antagonists (CTZ and YM) and the chemotherapeutic agent TZM

Combined therapy with the mGluR1 antagonists CTZ and YM (100 and 200 µM) and the chemotherapeutic agent TZM (200 µM) led to a significant stronger inhibition of mitochondrial activity of KRJ-I cells than single treatment (Table 18, Fig. 31 and 32). The strongest effect was reported on the third day of incubation. Similar results were obtained in experiments with P-STS cells after combined treatment with YM and TZM (Table 19, Fig. 33 and 34). TZM (200 µM) alone also caused a statistically significant reduction of mitochondrial activity.

Table 18 – Mitochondrial activity of KRJ-I cells after combined treatment with the mGluR1 antagonists and TZM
Effects on mitochondrial activity of KRJ-I cells after combined therapy with CTZ and YM (100 and 200 µM) and the chemotherapeutic agent TZM (200 µM). All results are relatively compared to a negative control (100%).

KRJ-I	day 1		day 2		day 3	
CTZ 200 µM	63,72%	**	59,17%	**	49,10%	**
CTZ 100 µM	72,19%	**	66,73%	**	51,49%	**
TZM 200 µM	74,75%	**	71,57%		63,21%	**
CTZ 200 µM + TZM 200 µM	53,08%	**	40,64%	**	30,52%	**
CTZ 100 µm + TZM 200 µM	63,54%	**	53,25%	*	33,40%	*
YM 200 µM	35,92%	**	31,47%	**	33,07%	**
YM 100 µM	71,46%	**	76,34%	*	88,54%	
TZM 200 µM	83,12%		72,54%	**	67,76%	*
YM 200 µM + TZM 200 µM	39,05%	**	31,55%	**	22,42%	**
YM 100 µM + TZM 100 µM	69,85%	**	65,15%	**	47,22%	**

Table 19 – Mitochondrial activity of SI-NET cells after combined treatment with YM and TZM
Effects on mitochondrial activity of P-STS cells after combined therapy with YM (100 and 200 µM) and the chemotherapeutic agent TZM (200 µM). All results are compared to a negative control (100%).

P-STS	day 1		day 2		day 3	
YM 200 µM	62,99%	*	53,62%	**	36,76%	**
YM 100 µM	77,25%	**	61,60%	**	44,77%	**
TZM 200 µM	98,62%		94,68%		117,14%	*
YM 200 µM + TZM 200 µM	61,93%	**	47,77%	**	29,50%	**
YM 100 µM + TZM 100 µM	70,07%	**	56,81%	**	36,64%	**

Mitochondrial activity SI-NETs – combined treatment

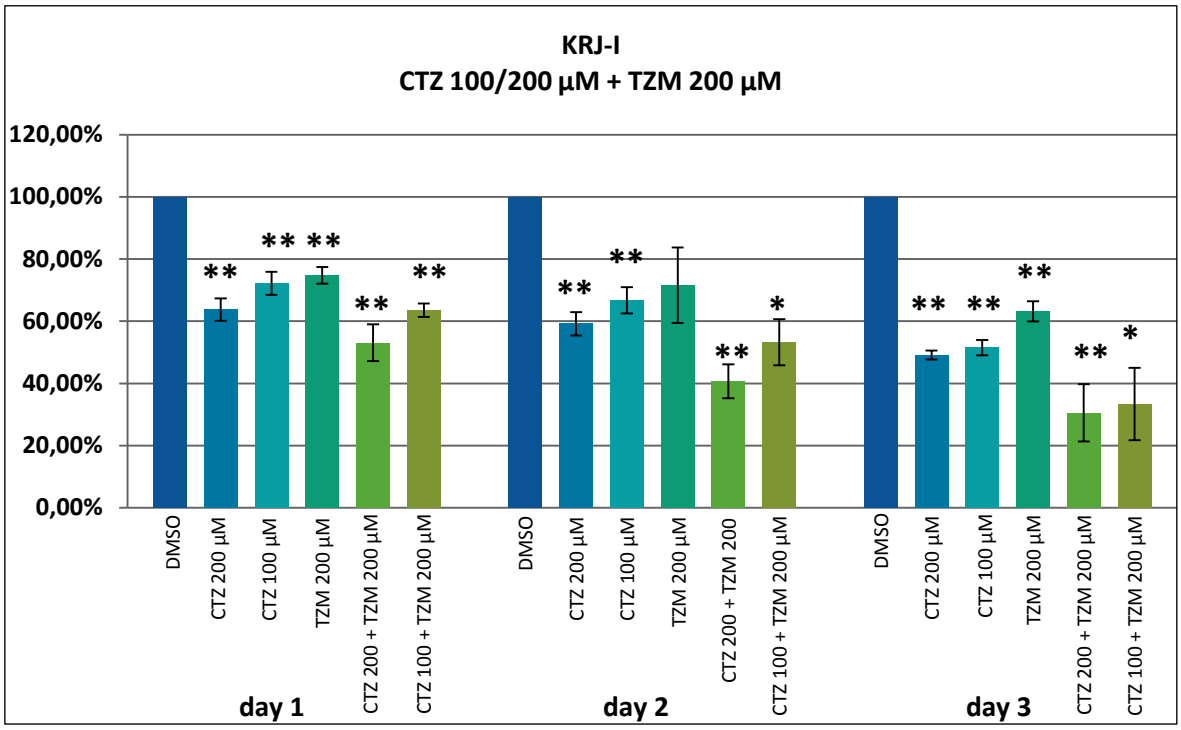

Fig. 31 – Mitochondrial activity of KRJ-I cells after combined treatment with CTZ and TZM
Results of the WST-1 assay compared to a negative control (100%)

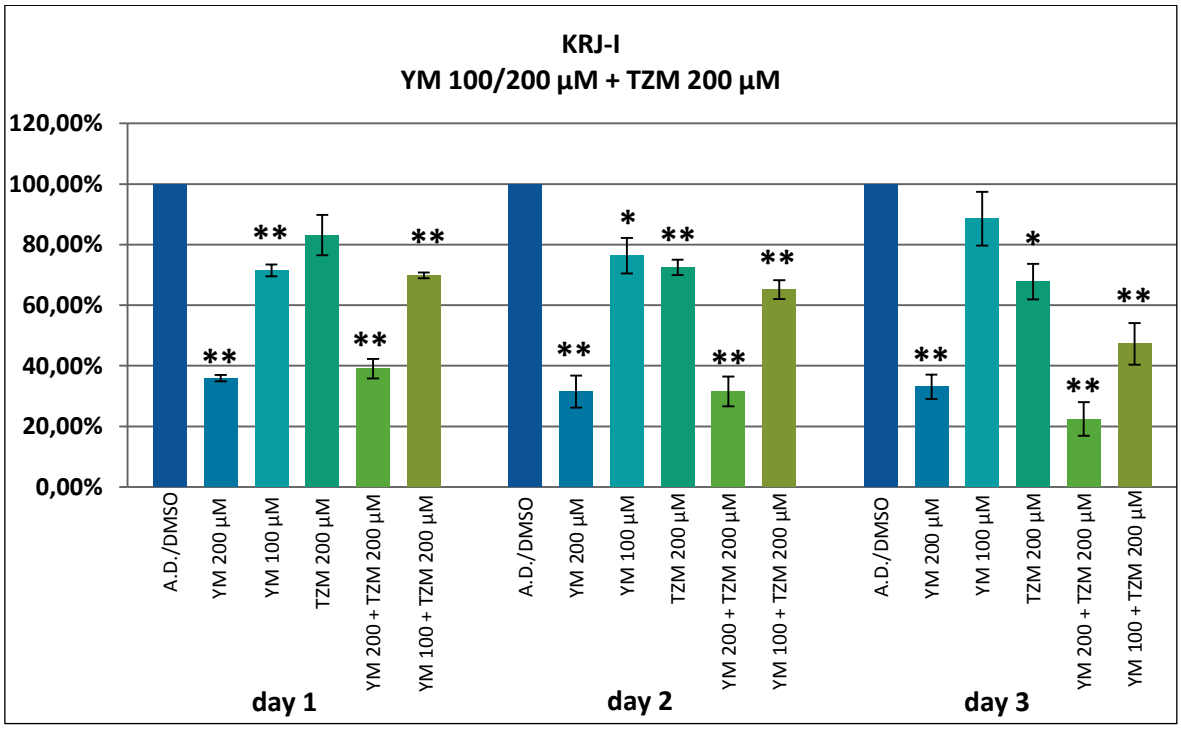

Fig. 32 – Mitochondrial activity of KRJ-I cells after combined treatment with YM and TZM
Results of the WST-1 assay compared to a negative control (100%). Similar effects were obtained in experiments with P-STS cells.

5.2 MTC cell lines

Single treatment with mGluR1 antagonists

Similar results were reported in experiments with MTC cells. Single treatment with the mGluR1 antagonists (100 and 200 µM) led to reduction of mitochondrial activity of MTC cells MTC-SK (Fig. 33 and 34) and SHER-I in a dose-dependent manner, whereby the dosage of 200 µM was the most effective (Table 20 and 21). In some experiments, lower concentrations caused higher mitochondrial activity compared to the negative control.

Table 20 – Effects of CTZ on mitochondrial activity of MTC cells
Mitochondrial activity of MTC-SK and SHER-I cells after single treatment with CTZ analysed by the WST-1 assay compared to a negative control (100%)

		CTZ 200 µM		CTZ 100 µM	
MTC-SK	**day 1**	66,07%	*	73,00%	*
	day 2	69,51%	**	87,28%	*
	day 3	73,07%	**	89,13%	**
SHER-I	**day 1**	34,07%	**	49,58%	**
	day 2	26,65%	**	46,12%	**
	day 3	29,06%	**	51,49%	**

Table 21 – Effects of YM on mitochondrial activity of MTC cells
Mitochondrial activity of MTC-SK and SHER-I cells after single treatment with YM analysed by the WST-1 assay compared to a negative control (100%)

		YM 200 µM		YM 100 µM	
MTC-SK	**day 1**	52,95%	*	100,32%	
	day 2	27,85%	**	81,60%	
	day 3	21,79%	**	79,69%	*
SHER-I	**day 1**	31,08%	**	68,55%	*
	day 2	21,47%	**	63,40%	*
	day 3	12,52%	**	76,73%	

Mitochondrial activity MTCs – single treatment

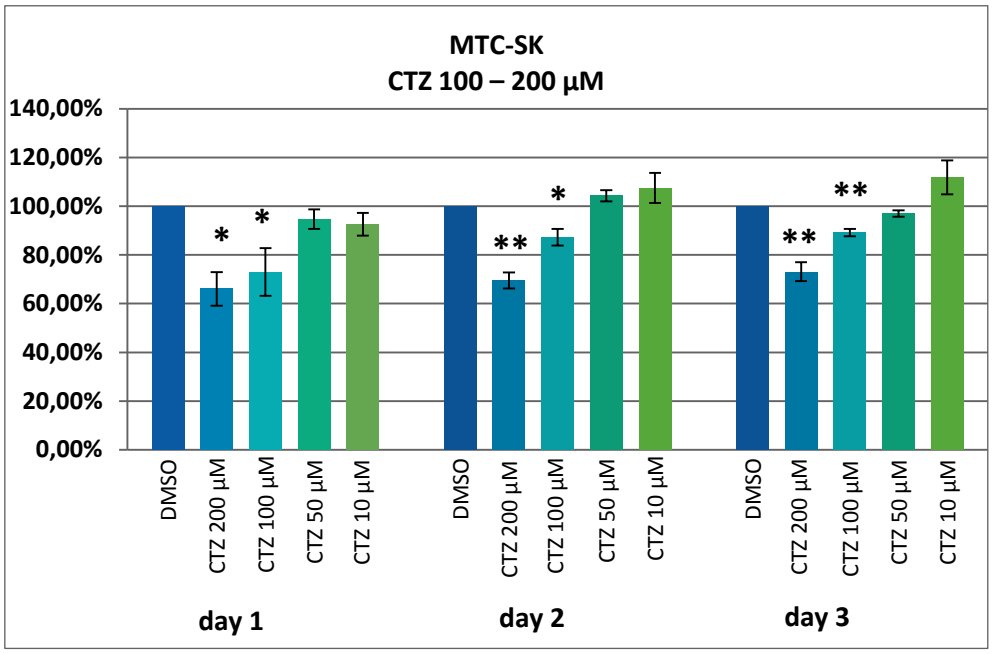

Fig. 33 – Mitochondrial activity of MTC-SK cells after single treatment with CTZ
Mitochondrial activity of MTC-SK cells after single treatment with CTZ analysed by the WST-1 assay, compared to a negative control (100%). Similar effects were obtained in experiments with SHER-I cells.

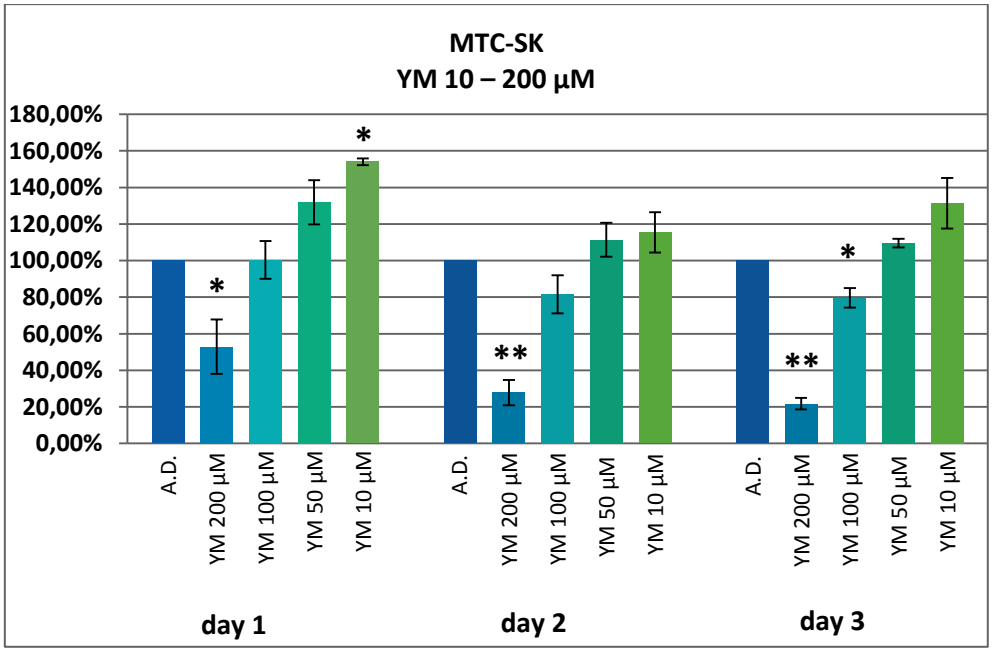

Fig. 34 – Mitochondrial activity of MTC-SK cells after single treatment with YM
Mitochondrial activity of SHER-I cells after single treatment with YM analysed by the WST-1 assay, compared to a negative control (100%). Similar effects were obtained in experiments with SHER-I cells.

Combined treatment with the mGluR1 antagonists (CTZ and YM) and the chemotherapeutic agent TZM

Combined therapy with the mGluR1 antagonists CTZ and YM (100 and 200 µM) and the chemotherapeutic agent TZM (200 µM) caused a stronger reduction of mitochondrial activity of MTC-SK cells than single treatment (Table 22, Fig. 35 and 36). Similar results were obtained in experiments with SHER-I cells (Table 23). TZM (200 µM) alone also caused a decreased mitochondrial activity.

Table 22 – Mitochondrial activity of MTC-SK cells after combined treatment with the mGluR1 antagonists and TZM

Effects on mitochondrial activity of MTC-SK cells after combined therapy with CTZ or YM (100 and 200 µM) and the chemotherapeutic agent TZM (200 µM). All results are compared to a negative control (100%).

MTC-SK	day 1		day 2		day 3	
CTZ 200 µM	58,69%	**	49,49%	**	48,50%	**
CTZ 100 µM	71,25%	**	60,93%	**	54,91%	**
TZM 200 µM	79,11%	**	68,12%	*	59,79%	*
CTZ 200 µM + TZM 200 µM	50,67%	**	37,52%	**	32,22%	**
CTZ 100 µm + TZM 200 µM	63,13%	**	53,06%	**	42,85%	**
YM 200 µM	44,95%	**	40,32%	**	45,11%	*
YM 100 µM	80,64%	*	84,31%		75,28%	
TZM 200 µM	67,02%	*	55,86%	*	42,51%	*
YM 200 µM + TZM 200 µM	38,69%	**	26,43%	**	21,04%	**
YM 100 µM + TZM 100 µM	71,69%		52,30%	**	30,82%	**

Table 23 – Mitochondrial activity of SHER-I cells after combined treatment with the mGluR1 antagonists and TZM

Effects on mitochondrial activity of SHER-I cells after combined therapy with CTZ or YM (100 and 200 µM) and the chemotherapeutic agent TZM (200 µM). All results are compared to a negative control (100%).

SHER-I	day 1		day 2		day 3	
CTZ 200 µM	56,90%	*	41,46%	**	42,51%	**
CTZ 100 µM	62,65%	*	54,05%	**	58,77%	**
TZM 200 µM	78,91%	**	84,48%	*	84,04%	
CTZ 200 µM + TZM 200 µM	56,37%	*	37,66%	**	37,54%	**
CTZ 100 µm + TZM 200 µM	69,81%	**	46,62%	**	50,16%	**
YM 200 µM	29,82%	**	17,45%	**	16,03%	**
YM 100 µM	53,18%	**	45,62%	**	51,09%	**
TZM 200 µM	84,41%		78,19%	*	79,56%	
YM 200 µM + TZM 200 µM	27,69%	**	19,59%	**	15,27%	**
YM 100 µM + TZM 100 µM	57,96%	*	41,94%	**	41,25%	**

Mitochondrial activity MTCs – combined treatment

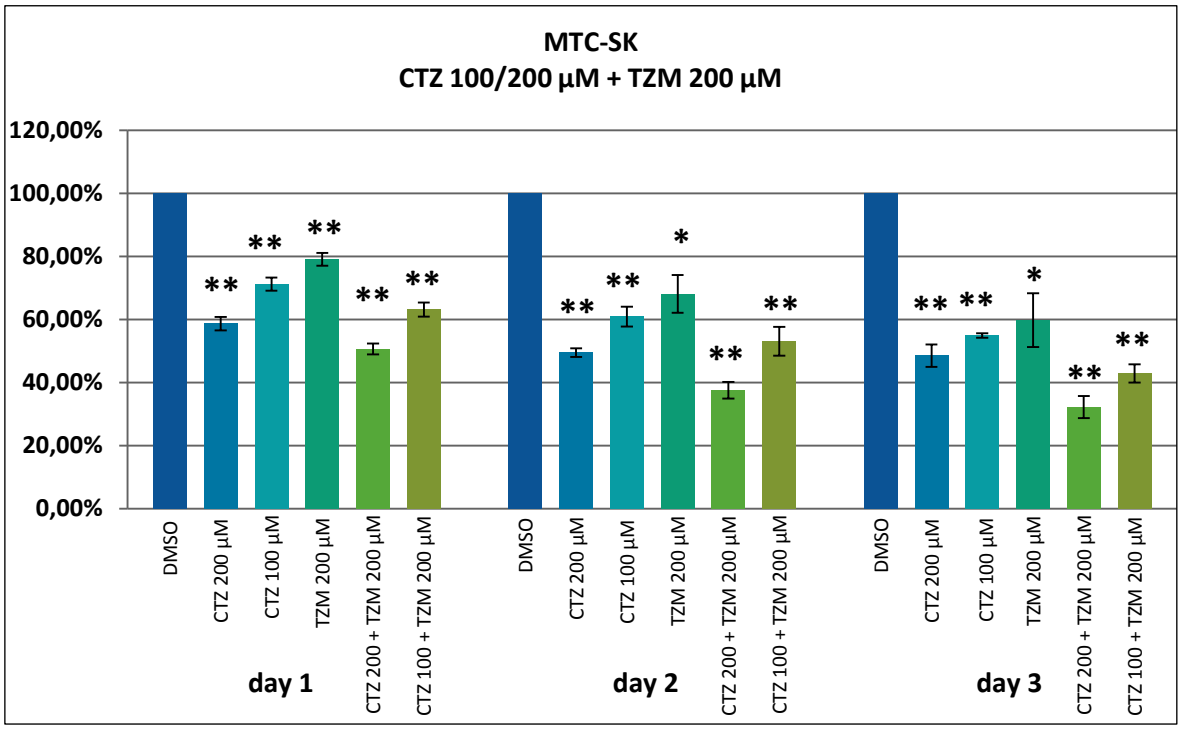

Fig. 35 – Mitochondrial activity of MTC-SK cells after combined treatment with CTZ and TZM
Mitochondrial activity of MTC-SK cells after combined treatment with CTZ analysed by the WST-1 assay, compared to a negative control (100%). Similar effects were obtained in experiments with SHER-I cells.

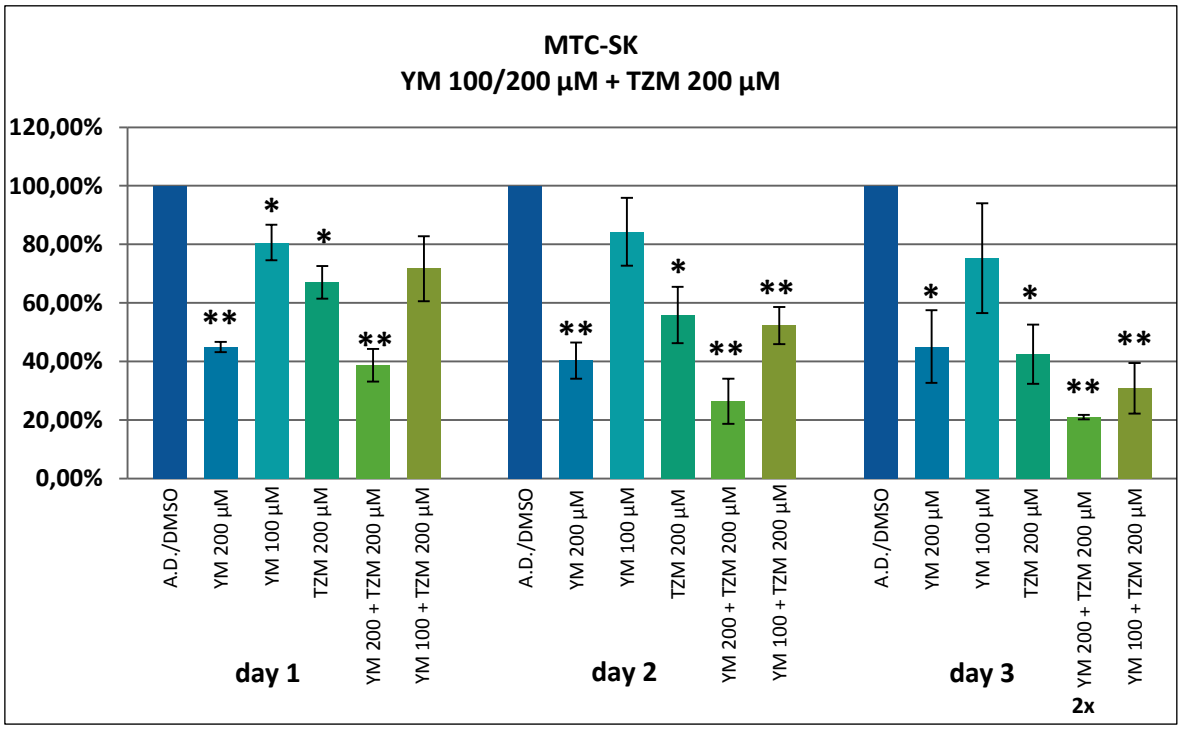

Fig. 36 – Mitochondrial activity of MTC-SK cells after combined treatment with YM and TZM
Mitochondrial activity of MTC-SK cells after combined treatment with YM and TZM analysed by the WST-1 assay, compared to a negative control (100%). Results marked with 2x refer to two experiments. Similar effects were obtained in experiments with SHER-I cells.

D. DISCUSSION

Neuroendocrine Tumors (NETs) form a heterogeneous group of neoplasms, including small intestinal NETs (SI-NETs) and medullary thyroid carcinomas (MTCs). As radio- and chemotherapy are usually ineffective, radical surgery is the only curative treatment option. To improve therapeutic outcome it is necessary to investigate new possible targets for anticancer therapy (1,7,54-56).

Glutamate is known as the most common excitatory neurotransmitter, but also plays a role in peripheral signalling (26,35,57). Negative allosteric modulation of glutamate receptors causes anticancer effects in different tumors (e.g. colon adenocarcinoma, breast and lung carcinoma) (28). Recent data suggest the metabotropic glutamate receptor 1 (mGluR1) as a possible target in tumor therapy (30).

Little is known about glutamate signalling in NETs, but the non-competitive, subtype-specific, mGluR1 antagonist CPCCOEt caused inhibition of tumor growth in medullary thyroid carcinoma (MTC) cell line MTC-SK (35). Objective of this study was to evaluate the therapeutic potential of mGluR1 antagonists in the treatment of NETs.

mGluR1 expression in NET cell lines

It is proven that glutamate receptors are not only expressed in the central nervous system, but also in peripheral tissues and tumor cells (35). For example, expression of mGluR1 is described in prostate cancer cells, but not in normal gland cells (29). Glutamate signalling plays a critical role in the development of melanoma (32,58-60), but there is a lack of knowledge about glutamate signalling in NETs. The expression of mGluR4 is described in papillary and medullary thyroid cancer (61). Normal enterochromaffin cells also express mGluR4, but not tumor cells (62). In this study, expression of the mGluR1 was detected in all tested cell lines. This underlines that mGluR1 is a possible target in tumor therapy of NETs. To provide the impact of mGluR1 expression on the development of neuroendocrine tumors, further investigations are required, for example, analysis of mGluR1 expression in enterochromaffin cells and parafollicular C-cells.

Inhibition of proliferation in all NET cells

Both tested mGluR1 antagonists, Cyclothiazide (CTZ) and YM-298198 (YM), influenced proliferation of several NET cells in a dose dependent manner, whereby the dosage of 200 µM was the most effective. CTZ and YM induced a stronger antiproliferative effect on KRJ-I, L-STS and H-STS cells than on P-STS cells. A reason therefore could be that P-STS cells are growing in monolayers and not in cell spheroids. Effects on MTC-SK and SHER-I cells were comparable to the effects of CPCCOEt on MTC-SK cells (35). It is remarkable that the antiproliferative effect of both mGluR1 antagonists affects all tested cell lines. This enhances the hypothesis that mGluR1 signalling plays a specific role in tumor biology of NETs.

Considering the desire to find apoptotic inducing agents as possible therapeutics in cancer therapy, further investigations are needed to examine whether treatment with the mGluR1 antagonists induces necrosis or apoptosis. The antiproliferative effect of CPCCOEt on melanoma cells appeared to be independent of apoptotic processes, since TUNEL analysis revealed that apoptosis-associated DNA strand breaks do not occur (33). However, detected cell shrinking in several NET cell lines (KRJ-I, L-STS, H-STS, MTC-SK and SHER-I) after treatment with CTZ and YM at the dosage of 200 µM could be an indicative of apoptotic cell death (63).

Reduced mitochondrial activity in NET cells

The results of the WST-1 assay show that both mGluR1 antagonists dose dependently reduced activity of the mitochondrial dehydrogenase in the cell samples. This correlates with a smaller amount of viable cells and confirms the abovementioned antiproliferative effect. The mGluR1 antagonist CPCCOEt did not affect cell viability of normal human skin fibroblasts (HF-SAR), which serve as non malignant control cells in other studies (59). Nevertheless, analysis of the effects of the mGluR1 antagonists CTZ and YM to normal enterochromaffin cells and parafollicular C-cells is an important outstanding investigation.

Synergistic effects of mGluR1 antagonists and the chemotherapeutic agent TZM

The mGluR1 antagonist CPCCOEt inhibited cell proliferation of melanoma cells, but also enhanced the antiproliferative effects of the anticancer agent docetaxel (33). The chemotherapeutic agent Temozolomide (TZM) showed promising effects in the treatment

of patients with NETs, alone as well as in combination with bevacizumab and capecitabine (9). In this study, TZM alone had an antiproliferative effect on all tested cell lines. The combined treatment with the mGluR1 antagonists CTZ and YM and the chemotherapeutic agent TZM led to a more pronounced effect in comparison with either treatment alone in several cell lines. Results of the WST-1 assay showed even stronger synergistic effects than the cell counting assay. The results of this *in vitro* study suggest the mGluR1 antagonists CTZ and YM as possible new substances for combined treatment.

Influence on morphology of NET cells

Additionally, morphological changes were detected. YM inhibited aggregate formation of all cell lines, which tend to build spheroid aggregates (KRJ-I, L-STS, H-STS, MTC-SK and SHER-I), but did not cause morphological changes in P-STS cells, which grow as slackly monolayer. Under the assumption, that there is a connection between the building of spheroid cell aggregates and insensitivity to radio- and chemotherapy (64) dissociation of cell spheroids could enhance response rates to cytotoxic drugs. CTZ did not affect cell spheroids in a comparable way, but caused smaller cell spheroids of KRJ-I and MTC-SK cells. Given the fact that CTZ and YM cause different effects on morphology, this may indicate that CTZ and YM could also activate different additional downstream signalling cascades.

Conclusion

Summarizing, all reported data provide evidences that the metabotropic glutamate receptor 1 is a possible target in anticancer therapy of drug resistant neuroendocrine tumors. Additionally, all results are due to a close interaction between the brain, neurotransmitters and tumor cells. This *in vitro* study cannot prove the efficiency of mGluR1 antagonists in *in vivo* treatment of NETs, but it builds the basis for further investigations to underline the reported antiproliferative effects, to explore tumor biology of NETs and for a better understanding of these intricate interactions.

E. REFERENCES

(1) Modlin IM, Kidd M, Latich I, Zikusoka MN, Shapiro MD. Current status of gastrointestinal carcinoids. Gastroenterology 2005 May;128(6):1717-1751.

(2) Yao JC, Hassan M, Phan A, Dagohoy C, Leary C, Mares JE, et al. One hundred years after "carcinoid": epidemiology of and prognostic factors for neuroendocrine tumors in 35,825 cases in the United States. J Clin Oncol 2008 Jun 20;26(18):3063-3072.

(3) Modlin IM, Lye KD, Kidd M. A 5-decade analysis of 13,715 carcinoid tumors. Cancer 2003 Feb 15;97(4):934-959.

(4) Ganetsky A, Bhatt V. Gastroenteropancreatic neuroendocrine tumors: update on therapeutics. Ann Pharmacother 2012 Jun;46(6):851-862.

(5) Modlin IM, Latich I, Kidd M, Zikusoka M, Eick G. Therapeutic options for gastrointestinal carcinoids. Clin Gastroenterol Hepatol 2006 May;4(5):526-547.

(6) Williams ED. Histogenesis of medullary carcinoma of the thyroid. J Clin Pathol 1966 Mar;19(2):114-118.

(7) American Thyroid Association Guidelines Task Force, Kloos RT, Eng C, Evans DB, Francis GL, Gagel RF, et al. Medullary thyroid cancer: management guidelines of the American Thyroid Association. Thyroid 2009 Jun;19(6):565-612.

(8) Griebeler ML, Gharib H, Thompson GB. Medullary thyroid carcinoma. Endocr Pract 2013 Jul-Aug;19(4):703-711.

(9) Naraev BG, Strosberg JR, Halfdanarson TR. Current status and perspectives of targeted therapy in well-differentiated neuroendocrine tumors. Oncology 2012;83(3):117-127.

(10) Bennett MR, Balcar VJ. Forty years of amino acid transmission in the brain. Neurochem Int 1999 Oct;35(4):269-280.

(11) Robinson MB, Coyle JT. Glutamate and related acidic excitatory neurotransmitters: from basic science to clinical application. FASEB J 1987 Dec;1(6):446-455.

(12) Skerry TM, Genever PG. Glutamate signalling in non-neuronal tissues. Trends Pharmacol Sci 2001 Apr;22(4):174-181.

(13) Hinoi E, Takarada T, Ueshima T, Tsuchihashi Y, Yoneda Y. Glutamate signaling in peripheral tissues. Eur J Biochem 2004 Jan;271(1):1-13.

(14) Kew JN, Kemp JA. Ionotropic and metabotropic glutamate receptor structure and pharmacology. Psychopharmacology (Berl) 2005 Apr;179(1):4-29.

(15) Willard SS, Koochekpour S. Glutamate, glutamate receptors, and downstream signaling pathways. Int J Biol Sci 2013 Sep 22;9(9):948-959.

(16) Schoepp DD, Jane DE, Monn JA. Pharmacological agents acting at subtypes of metabotropic glutamate receptors. Neuropharmacology 1999 Oct;38(10):1431-1476.

(17) Kniazeff J, Bessis AS, Maurel D, Ansanay H, Prezeau L, Pin JP. Closed state of both binding domains of homodimeric mGlu receptors is required for full activity. Nat Struct Mol Biol 2004 Aug;11(8):706-713.

(18) Kunishima N, Shimada Y, Tsuji Y, Sato T, Yamamoto M, Kumasaka T, et al. Structural basis of glutamate recognition by a dimeric metabotropic glutamate receptor. Nature 2000 Oct 26;407(6807):971-977.

(19) Hermans E, Challiss RA. Structural, signalling and regulatory properties of the group I metabotropic glutamate receptors: prototypic family C G-protein-coupled receptors. Biochem J 2001 Nov 1;359(Pt 3):465-484.

(20) Kew JN. Positive and negative allosteric modulation of metabotropic glutamate receptors: emerging therapeutic potential. Pharmacol Ther 2004 Dec;104(3):233-244.

(21) Ott D, Floersheim P, Inderbitzin W, Stoehr N, Francotte E, Lecis G, et al. Chiral resolution, pharmacological characterization, and receptor docking of the noncompetitive mGlu1 receptor antagonist (+/-)-2-hydroxyimino- 1a, 2-dihydro-1H-7-oxacyclopropa[b]naphthalene-7a-carboxylic acid ethyl ester. J Med Chem 2000 Nov 16;43(23):4428-4436.

(22) Litschig S, Gasparini F, Rueegg D, Stoehr N, Flor PJ, Vranesic I, et al. CPCCOEt, a noncompetitive metabotropic glutamate receptor 1 antagonist, inhibits receptor signaling without affecting glutamate binding. Mol Pharmacol 1999 Mar;55(3):453-461.

(23) Surin A, Pshenichkin S, Grajkowska E, Surina E, Wroblewski JT. Cyclothiazide selectively inhibits mGluR1 receptors interacting with a common allosteric site for non-competitive antagonists. Neuropharmacology 2007 Mar;52(3):744-754.

(24) Kohara A, Toya T, Tamura S, Watabiki T, Nagakura Y, Shitaka Y, et al. Radioligand binding properties and pharmacological characterization of 6-amino-N-cyclohexyl-N,3-dimethylthiazolo[3,2-a]benzimidazole-2-carboxamide (YM-298198), a high-affinity, selective, and noncompetitive antagonist of metabotropic glutamate receptor type 1. J Pharmacol Exp Ther 2005 Oct;315(1):163-169.

(25) Partin KM, Fleck MW, Mayer ML. AMPA receptor flip/flop mutants affecting deactivation, desensitization, and modulation by cyclothiazide, aniracetam, and thiocyanate. J Neurosci 1996 Nov 1;16(21):6634-6647.

(26) Julio-Pieper M, Flor PJ, Dinan TG, Cryan JF. Exciting times beyond the brain: metabotropic glutamate receptors in peripheral and non-neural tissues. Pharmacol Rev 2011 Mar;63(1):35-58.

(27) Shin SS, Martino JJ, Chen S. Metabotropic glutamate receptors (mGlus) and cellular transformation. Neuropharmacology 2008 Sep;55(4):396-402.

(28) Rzeski W, Turski L, Ikonomidou C. Glutamate antagonists limit tumor growth. Proc Natl Acad Sci U S A 2001 May 22;98(11):6372-6377.

(29) Koochekpour S, Majumdar S, Azabdaftari G, Attwood K, Scioneaux R, Subramani D, et al. Serum glutamate levels correlate with Gleason score and glutamate blockade decreases

proliferation, migration, and invasion and induces apoptosis in prostate cancer cells. Clin Cancer Res 2012 Nov 1;18(21):5888-5901.

(30) Nicoletti F, Arcella A, Iacovelli L, Battaglia G, Giangaspero F, Melchiorri D. Metabotropic glutamate receptors: new targets for the control of tumor growth? Trends Pharmacol Sci 2007 May;28(5):206-213.

(31) Li S, Huang S, Peng SB. Overexpression of G protein-coupled receptors in cancer cells: involvement in tumor progression. Int J Oncol 2005 Nov;27(5):1329-1339.

(32) Pollock PM, Cohen-Solal K, Sood R, Namkoong J, Martino JJ, Koganti A, et al. Melanoma mouse model implicates metabotropic glutamate signaling in melanocytic neoplasia. Nat Genet 2003 May;34(1):108-112.

(33) Haas HS, Pfragner R, Siegl V, Ingolic E, Heintz E, Schraml E, et al. The non-competitive metabotropic glutamate receptor-1 antagonist CPCCOEt inhibits the in vitro growth of human melanoma. Oncol Rep 2007 Jun;17(6):1399-1404.

(34) Speyer CL, Smith JS, Banda M, DeVries JA, Mekani T, Gorski DH. Metabotropic glutamate receptor-1: a potential therapeutic target for the treatment of breast cancer. Breast Cancer Res Treat 2012 Apr;132(2):565-573.

(35) Haas HS, Linecker A, Pfragner R, Sadjak A. Peripheral glutamate signaling in head and neck areas. Head Neck 2010 Nov;32(11):1554-1572.

(36) Tatar Z, Thivat E, Planchat E, Gimbergues P, Gadea E, Abrial C, et al. Temozolomide and unusual indications: review of literature. Cancer Treat Rev 2013 Apr;39(2):125-135.

(37) Quirbt I, Verma S, Petrella T, Bak K, Charette M, Members of the Melanoma Disease Site Group of Cancer Care Ontario's Program in Evidence-Based Care. Temozolomide for the treatment of metastatic melanoma. Curr Oncol 2007 Feb;14(1):27-33.

(38) Stupp R, Hegi ME, Mason WP, van den Bent MJ, Taphoorn MJ, Janzer RC, et al. Effects of radiotherapy with concomitant and adjuvant temozolomide versus radiotherapy alone on survival in glioblastoma in a randomised phase III study: 5-year analysis of the EORTC-NCIC trial. Lancet Oncol 2009 May;10(5):459-466.

(39) Jalali R, Basu A, Gupta T, Munshi A, Menon H, Sarin R, et al. Encouraging experience of concomitant Temozolomide with radiotherapy followed by adjuvant Temozolomide in newly diagnosed glioblastoma multiforme: single institution experience. Br J Neurosurg 2007 Dec;21(6):583-587.

(40) Jiang G, Li RH, Sun C, Jia HY, Lei TC, Liu YQ. Efficacy and safety between temozolomide alone and temozolomide-based double therapy for malignant melanoma: a meta-analysis. Tumour Biol 2014 Jan;35(1):315-322.

(41) Ekeblad S, Sundin A, Janson ET, Welin S, Granberg D, Kindmark H, et al. Temozolomide as monotherapy is effective in treatment of advanced malignant neuroendocrine tumors. Clin Cancer Res 2007 May 15;13(10):2986-2991.

(42) Koumarianou A, Antoniou S, Kanakis G, Economopoulos N, Rontogianni D, Ntavatzikos A, et al. Combination treatment with metronomic temozolomide, bevacizumab and long-acting octreotide for malignant neuroendocrine tumours. Endocr Relat Cancer 2012 Jan 9;19(1):L1-4.

(43) Saif MW, Kaley K, Brennan M, Garcon MC, Rodriguez G, Rodriguez T. A retrospective study of capecitabine/temozolomide (CAPTEM) regimen in the treatment of metastatic pancreatic neuroendocrine tumors (pNETs) after failing previous therapy. JOP 2013 Sep 10;14(5):498-501.

(44) Strosberg JR, Fine RL, Choi J, Nasir A, Coppola D, Chen DT, et al. First-line chemotherapy with capecitabine and temozolomide in patients with metastatic pancreatic endocrine carcinomas. Cancer 2011 Jan 15;117(2):268-275.

(45) Welin S, Sorbye H, Sebjornsen S, Knappskog S, Busch C, Oberg K. Clinical effect of temozolomide-based chemotherapy in poorly differentiated endocrine carcinoma after progression on first-line chemotherapy. Cancer 2011 Oct 15;117(20):4617-4622.

(46) Pfragner R, Wirnsberger G, Niederle B, Behmel A, Rinner I, Mandl A, et al. Establishment of a continuous cell line from a human carcinoid of the small intestine (KRJ-I). Int J Oncol 1996 Mar;8(3):513-520.

(47) Kidd M, Eick GN, Modlin IM, Pfragner R, Champaneria MC, Murren J. Further delineation of the continuous human neoplastic enterochromaffin cell line, KRJ-I, and the inhibitory effects of lanreotide and rapamycin. J Mol Endocrinol 2007 Feb;38(1-2):181-192.

(48) Pfragner R, Behmel A, Hoger H, Beham A, Ingolic E, Stelzer I, et al. Establishment and characterization of three novel cell lines - P-STS, L-STS, H-STS - derived from a human metastatic midgut carcinoid. Anticancer Res 2009 Jun;29(6):1951-1961.

(49) Pfragner R, Hofler H, Behmel A, Ingolic E, Walser V. Establishment and characterization of continuous cell line MTC-SK derived from a human medullary thyroid carcinoma. Cancer Res 1990 Jul 1;50(13):4160-4166.

(50) Stadler G, Wieser M, Streubel B, Stift A, Friedl J, Gnant M, et al. Low telomerase activity: possible role in the progression of human medullary thyroid carcinoma. Eur J Cancer 2008 Apr;44(6):866-875.

(51) Chomczynski P, Sacchi N. Single-step method of RNA isolation by acid guanidinium thiocyanate-phenol-chloroform extraction. Anal Biochem 1987 Apr;162(1):156-159.

(52) Pfaffl MW. A new mathematical model for relative quantification in real-time RT-PCR. Nucleic Acids Res 2001 May 1;29(9):e45.

(53) Pfragner R, Flicker K, Hofer D, Schwach G, Fuchs R, Haas H, et al. Establishment and application of cell lines from medullary thyroid carcinoma. European Thyroid Journal, Launching Issue September 2011, 35th Annual Meeting of the European Thyroid Association 2011.

(54) Oberg K, Casanovas O, Castano JP, Chung D, Delle Fave G, Denefle P, et al. Molecular pathogenesis of neuroendocrine tumors: implications for current and future therapeutic approaches. Clin Cancer Res 2013 Jun 1;19(11):2842-2849.

(55) Castano JP, Sundin A, Maecke HR, Villabona C, Vazquez-Albertino R, Navarro E, et al. Gastrointestinal neuroendocrine tumors (NETs): new diagnostic and therapeutic challenges. Cancer Metastasis Rev 2014 Jan 5.

(56) Kebebew E, Ituarte PH, Siperstein AE, Duh QY, Clark OH. Medullary thyroid carcinoma: clinical characteristics, treatment, prognostic factors, and a comparison of staging systems. Cancer 2000 Mar 1;88(5):1139-1148.

(57) Gill SS, Pulido OM. Glutamate receptors in peripheral tissues: current knowledge, future research, and implications for toxicology. Toxicol Pathol 2001 Mar-Apr;29(2):208-223.

(58) Marin YE, Chen S. Involvement of metabotropic glutamate receptor 1, a G protein coupled receptor, in melanoma development. J Mol Med (Berl) 2004 Nov;82(11):735-749.

(59) Haas HS, Pfragner R, Siegl V, Ingolic E, Heintz E, Schraml E, et al. The non-competitive metabotropic glutamate receptor-1 antagonist CPCCOEt inhibits the in vitro growth of human melanoma. Oncol Rep 2007 Jun;17(6):1399-1404.

(60) Namkoong J, Shin SS, Lee HJ, Marin YE, Wall BA, Goydos JS, et al. Metabotropic glutamate receptor 1 and glutamate signaling in human melanoma. Cancer Res 2007 Mar 1;67(5):2298-2305.

(61) Stepulak A, Luksch H, Gebhardt C, Uckermann O, Marzahn J, Sifringer M, et al. Expression of glutamate receptor subunits in human cancers. Histochem Cell Biol 2009 Oct;132(4):435-445.

(62) Kidd M, Modlin IM, Gustafsson BI, Drozdov I, Hauso O, Pfragner R. Luminal regulation of normal and neoplastic human EC cell serotonin release is mediated by bile salts, amines, tastants, and olfactants. Am J Physiol Gastrointest Liver Physiol 2008 Aug;295(2):G260-72.

(63) Bortner CD, Cidlowski JA. Apoptotic volume decrease and the incredible shrinking cell. Cell Death Differ 2002 Dec;9(12):1307-1310.

(64) Hofer D, Schwach G, Ghaffari Tabrizi-Wizsy N, Sadjak A, Sturm S, Stuppner H, et al. Christia vespertilionis plant extracts as novel antiproliferative agent against human neuroendocrine tumor cells. Oncol Rep 2013 Jun;29(6):2219-2226.

F. LIST OF ABBREVIATIONS

5-HT	serotonin
A.D.	aqua bidest
Ala	alanine
AMPA	α-amino-3-hydroxy-5-methyl-4-isoazolepropionic acid
BAN	4-bromoanisole
BAY36-7620	(3aS,6aS)-6a-naphthalen-2-ylmethyl-5-methyliden-hexahydro-cyclopental[c]furan-1-on
bp	base pairs
Ca^{++}	calcium
cDNA	complementary deoxyribonucleic acid
CNS	central nervous system
CPCCOEt	7-(hydroxyimino)cyclopropa[b]chromen-1a-carboxylate ethyl ester
CRD	cysteine-rich domain
CTZ	Cyclothiacide, 3-(5-bicyclo[2.2.1]hept-2-enyl)-6-chloro-1,1-dioxo-3,4-dihydro-2H-1λ6,2,4-benzothiadiazine-7-sulfonamide
DAG	diacylglycerol
DMSO	dimethylsulfoxid
DNA	desoxyribonucleic acid
EC	enterochromaffin cells
EGFR	epidermal growth factro receptor
ELISA	enzyme linked immunosorbent assay
ERK	extracellular-signal related kinase
FBS	foetal bovine serum
GABA	gamma amino butyric acid
GPCR	guanine nucleotide-binding protein coupled receptor
G-protein	guanine nucleotide-binding protein
HBMC	human Bowes melanoma cell line

iGluR	ionotropic glutamate receptor
IP3	inositol 1,4,5-trisphosphate
K^+	kalium
MAPK	mitogen activated protein kinase
MEN	multiple endocrine neoplasia
mGluR	metabotropic glutamte receptor
MTC	medullary thyroid cancer
mTOR	mammalian target of rapamycin
n15006	human melanoma cell line
Na^+	natrium
NET	neuroendocrine tumor
NMDA	N-methyl-D-aspartate
NTP	nucleoside 5´-triphosphates
PLC	phospholipase C
qPCR	quantitative polymerase chain reaction
RET	rearranged during transfection proto-oncogene
RNA	ribonucleic acid
RT-PCR	reverse transcription polymerase chain reaction
SCID	severe combined immunodeficiency
SERT	serotonin transporter
SI-NET	small intestinal neuroendocrine tumors
TAE	tris-acetate-EDTA
Thr	threonine
TNBC	breast cancer cell line
TZM	Temozolomide
VEGF	vascular endothelial growth factor
VFT	venus flytrap domain
VMAT1	Vesicular monoamine transporter 1
WST-1	water-soluble tetrazolium salt 1
YM	YM-298198, 6-amino-N-cyclohexyl-N,3-dimethylthiazolo[3,2-a]benzimidazole-2-carboxamide

G. LIST OF FIGURES

H. LIST OF TABLES

I. APPENDIX: CONGRESS CONTRIBUTIONS

1. Abstract for OEGMBT 2012

The following abstract was accepted as a poster for the 4th OEGMBT Annual Meeting 2012 held from September, 17th- 19th 2012 in Graz (Austria).

Glutamate receptor antagonists as a new targeted therapy of neuroendocrine tumors

Rohrer K[1], Haas HS[1], Pfragner R[1], Ghaffari Tabrizi-Wizsy N[1], Allard N[1], Horwath C[1], Lueftenegger I[1], Rinner B[2], Sadjak A[1]

[1]*Institute of Pathophysiology and Immunology, Center of Molecular Medicine, Medical University of Graz, Heinrichstrasse 31A, 8010 Graz, Austria.*

[2]*Core Facility Flow Cytometry, Center for Medical Research, Medical University of Graz, Stiftingtalstrasse 24, 8010 Graz, Austria*

Background: Standard chemotherapy and radiotherapy are used for treatment of neuroendocrine tumors. However, response rates are low. Therefore, new research concepts for novel treatment options are needed. In the last years we found that glutamate receptor antagonists influence tumor growth and cell activity of different malignancies, including neuroendocrine tumors. This suggests a possibility of a new target in cancer therapy.

Methods: Cell counting is performed using the CASY-1® Cell Counter & Analyser. Metabolic cell activity is measured by the colorimetric Cell Proliferation Assay WST-1. Metabotropic glutamate receptor expression is examined by PCR analyses.

Results: PCR analyses of a human medullary thyroid carcinoma cell line (MTC-SK) and different human midgut carcinoid cell lines (KRJ-I, P-STS, L-STS, H-STS) revealed expression of glutamate receptor subtypes. Two subtype-specific, non-competitive, metabotropic glutamate-receptor-1 (mGluR1) antagonists (Cyclothiazide, YM298198) reduced growth and metabolic cell activity of the aforementioned neuroendocrine cell lines in a dose-dependent way. Same treatment did not influence normal human fibroblasts.

Conclusion: Our results show that glutamate receptors are a potential target for neuroendocrine tumor therapy.

2. Abstract for ISC 2013

The following abstract was accepted for an oral presentation at the 1st International Student Congress held from July, 4th- 6th 2013 in Graz (Austria).

Effects of Metabotropic-Glutamate-Receptor-1 Antagonists on Neuroendocrine Tumors

K.Rohrer, N.Ghaffari Tabrizi-Wizsy, H.S.Haas, C.Horwath, N.Allard, G.Schwach, R.Pfragner, A.Sadjak

Background: Treatment regimens for Neuroendocrine Tumors (NETs) are still insufficient, because response rates to standard chemotherapy and radiotherapy are low. Radical surgery is the only curative option.

Glutamate is an important excitatory neurotransmitter. Glutamate receptors, however, are not only expressed in neuronal, but also in peripheral tissues. They represent a possible target for cancer therapy, because glutamate-receptor antagonists have shown to suppress tumor growth, i.e. in melanoma cells.

Aims: New therapeutic strategies for the treatment of NETs are needed. Objective of this study is the analysis of metabotropic-glutamate-receptor-1 (mGluR1) as a possible target for cancer therapy. We aim to evaluate the influence of mGluR1 antagonists on proliferation, cell size and mitochondrial activity of neuroendocrine cell lines.

Methods: Different suspension cell lines of NETs are applied: human medullary thyroid carcinoma cell line (MTC-SK) and different human midgut carcinoid cell lines (KRJ-I, P-STS, L-STS, H-STS). All mentioned cell lines are cultivated in F12/M199 medium and treated with increasing concentrations (10µM, 50µM, 100µM and 200µM) of Cyclothiazide (CTZ) and YM298198 (YM). Both are subtype-specific, non-competitive mGluR1-antagonists. Within the following three days effects on proliferation, cell size and mitochondrial activity are evaluated using the CASY-1® Cell Counter & Analyser and the colorimetric Cell Proliferation Assay WST-1.
Furthermore, effects of the combination of mGluR1-antagonists and the chemotherapeutical agent Temozolomide (TZM) are analyzed under the same test conditions. TZM is a DNA methylating anti-cancer agent.
For detection of mGluR1 expression qualitative and quantitative PCR analyses are performed.
The results are statistically interpreted via t-test.

Results: Real Time PCR reveals the expression of mGluR1 in P-STS, L-STS, H-STS, KRJ-I and MTC-SK cells.
CTZ and YM suppressed proliferation and mitochondrial activity in a dose dependent way in all aforementioned cell lines. First results of the combination therapy with TZM suggest a synergistic inhibition of proliferation.

Conclusion: Our results clearly indicate that mGluR1-antagonists suppress the growth and mitochondrial activity of neuroendocrine tumor cells, *in vitro*, which makes them to possible targets in cancer therapy. Additionally, it refers to non-synaptic effects of glutamate receptors in peripheral tissues. For a better understanding of the molecular pathways more detailed examinations are needed.

Impact on medicine: Cancer causes death. In some cases standard therapy strategies reach their limits, but targeted therapy can improve the outcome. The task of basic research is to find new possible targets. This we want to achieve in our study.